

Characterizing the accelerated mass loss of the western Nyainqentanglha glaciers ~~in recent~~over the last 40 years

Shuhong Wang<sup>1,2</sup>, Jintao Liu<sup>1,2\*</sup>,

<sup>1</sup>State Key Laboratory of Hydrology-Water Resources and Hydraulic Engineering, Hohai University, Nanjing 210098, People's Republic of China;

<sup>2</sup> College of Hydrology and Water Resources, Hohai University, Nanjing 210098, People's Republic of China

\* Correspondence: jtliau@hhu.edu.cn; Tel.: +86-025-83787803

Abstract:

~~Accelerated~~ Glacier retreat ~~are breaking~~is changing the ~~inherent~~water regimes of ~~water~~balance on the Tibetan Plateau (TP) ~~under as the region's global warming~~climate changes, but there ~~remain~~There are still substantial gaps in quantification of regional glacier ~~changes as the main~~component of the water balance equation loss due to the difficulty of ~~making direct~~high-mountain ~~Asia glacier~~observations. Here, we assess 40 years of changes in the glaciers ~~changes of~~with the West Nyainqentanglha Range (WNT) ~~over the past 40 years that~~was assessed, where glaciers supply meltwater to ~~the densely-populated~~Lhasa River basin ~~which is the most densely-populated~~catchment and Nam Co Lake, ~~which is~~the second largest endorheic lake on the TP. We ~~have derived~~mapped glacier extent in 1976, 2000, 2014, and 2020 based on Landsat MSS/ETM+/OLI scenes and quantified changes in ice thickness during the intervals 1976–2000 and 2000–2020 using declassified KH-9 images, ~~the~~Shuttle Radar Topography Mission DEM (2000), and modern stereo satellite imagery. Results ~~revealed show~~that the glacier area retreat rate during 2000 to 2020 ( $1.17\% \text{ a}^{-1}$ ) was more than twice ~~as much as~~that from 1976 to 2000 ( $0.54\% \text{ a}^{-1}$ ). Similarly, ~~the our geodetic~~glacier mass balance ~~observations from 2000 to 2020 (of~~ $-0.37 \pm 0.15 \text{ m w.e. a}^{-1}$  from 2000 to 2020, ~~compared to~~was more negative than that from 1976 to 2000 ( $-0.26 \pm 0.09 \text{ m w.e. a}^{-1}$  ~~from 1976 to 2000~~) ~~due to the intensified glacier melting after 2014~~support ~~and our extraction results were~~reasonable compared with previous ~~but less comprehensive~~studies that indicate accelerating mass loss over this period, and we identify particularly intense melting after 2014. The spatial and temporal heterogeneity of glacier changes can ~~likely~~be partially explained by ~~local variations in~~climate change temperature and precipitation forcing in this region, ~~an apparent reduction in the~~melt-reducing role of debris cover, and an increasing influence of ice marginal lakes on glacier retreat, rates in the 2000–2020 period. Besides, during 2000–2020, ~~proglacial lakes played a more~~significant role in promoting glacier melting relative to 1976–2000, while debris cover played a weaker role in inhibiting glacier melting compared that of 1976–2000. The mass balance of debris-covered glaciers slightly negative than that of debris free glaciers during 2000–2020 indicated an advanced stage of glacier evolution. Additionally, ~~on average across the glacier population, steeper~~slopes were associated with it was found that the glacier area on steep slopes retreated faster areal retreat ~~than that on gentle slopes, while the but slower~~thickness thinning rates, while ~~on steep~~slopes was smaller than that on gentle slopes. The control of the influence of aspect on glacier area shrinkage retreat and thickness thinning was inconsistent ~~and temporal heterogeneous~~through time.

1. Introduction

Known as the “Water Tower of Asia”, the Tibetan Plateau (TP) is the source ~~area~~of several of Asia's ~~main-major~~major rivers (Bolch et al., 2010). Glacial melt on the TP plays ~~an important~~a pivotal role in water supply for downstream populations, agriculture and industries in these rivers (Pritchard, 2019; Viviroli et al., 2007). ~~Under~~Recent decades ~~of global warming~~climate change

批注 [HP-B1]: Can you add uncertainties +/- here?

批注 [HP-B2]: ...and here.

批注 [HP-B3]: I have reworded this because these thinning rates technically agree within their uncertainty range.

have boosted river runoff-discharge has by increasing runoff from as a result of accelerated shrinking glaciers (Lin et al., 2020; Yao et al., 2007; Zhang et al., 2011), but ~~it~~ this boost will eventually decrease as glacier area declines due to the decrease of the amount of glaciers on TP (Zhao et al., 2019). The sensitivity of ice loss to climate change is variable and often poorly known, however, being a function of ~~Since runoff tipping point is related to~~ glacier size, hypsometry, aspect, debris cover, and the presence of proglacial lakes and ice cliffs, for example glacier melting rate, precipitation and other factors. Combined with uncertainties in ice thickness and future climate scenarios, the occurrence time timing of 'peak water' and the subsequent decline in runoff of tipping point is still controversial remains a key unknown (Ding et al., 2020; Maurer et al., 2019; Su et al., 2016; Zhao et al., 2019). It ~~therefore, estimates of glacier changes are remains~~ therefore, estimates of glacier changes are remains critical to monitor and analyse glacier change to improving our understanding of its climate drivers, and thus to assess resulting its impacts on glacier-fed river basins (Immerzeel et al., 2020).

The WNT, in the south-eastern TP (Figure 1), is located in the transition zone between the two large-scale atmospheric circulation patterns characterised respectively by dominant westerly winds and the Indian summer monsoon. It holds an abundance of glaciers and glacier-fed lakes, notably Nam Co Lake in the northwest WNT, where recent intensified melting of glaciers in the WNT is the main reason for rising water levels (Bolch et al., 2010). The number and area of supraglacial lakes (of  $>0.0036 \text{ km}^2$ ) in the WNT also increased between 1976 and 2018, by 56% and 35% respectively, due to the increase in glacial meltwater (Luo et al., 2020). Furthermore, Zhou et al. (2013) revealed a water imbalance in Nam Co Basin based on the measured mass balance data of Zhadang Glacier and other hydrological observation data from 2007 to 2011. In the relatively densely-populated Lhasa Basin located on the TP in the southeast of WNT, Lin et al. (2020) also found a water imbalance using the first and second Chinese glacier inventories of 1960 and 2009. Despite these extensive changes and large affected population, logistical limitations have meant that in-situ glacier mass balance records are biased towards only a few low-lying, small glaciers that are unlikely to be representative of the broader region (Kääb et al., 2012; Li & Lin, 2017; Yao et al., 2012). Detailed investigation of the WNT glacier area and mass balance on a longer time scale is therefore a high priority.

Compared with the interpolation of sparse in-situ measurements and physical glacier change models, satellites can observations are more effective in surveying large scale glaciers change over much larger areas in of such remote and harsh areas terrain (Wang et al., 2021). In recent years, our understanding of the state of the glaciers state on the TP glaciers has been greatly improved by the increasing coverage and accuracy of multi-source remote sensing observations, such as the of glacier area, volume and mass change from KH-9 (Hexagon military satellites), Landsat, ASTER, the ICESat (Ice, Cloud, and land Elevation Satellite) altimetry mission, the GRACE gravimetry mission, and other Digital Elevation Models (DEMs) constructed by current space-geodetic techniques (Guo et al., 2015; Kääb et al., 2012; Wang et al., 2021; Zhou et al., 2018). For instance, Based on the KH-9 images and SRTM, for example, Zhou et al. (2018) found that glaciers in the northwest of the TP have thinned less rapidly ( $-0.11 \pm 0.13 \text{ m w.e. a}^{-1}$  to  $0.02 \pm 0.10 \text{ m w.e. a}^{-1}$ ) have shown a less negative compared to than those in the southeast part ( $-0.30 \pm 0.12 \text{ m w.e. a}^{-1}$  to  $-0.11 \pm 0.14 \text{ m w.e. a}^{-1}$ ) from the mid-1970s to 2000. Brun et al. (2018) employed ASTER DEMs and showed that glacier mass balances on High Mountain Asia vary from  $-0.62 \pm 0.23 \text{ m w.e. a}^{-1}$  in eastern Nyainqentanglha to  $+0.14 \pm 0.08 \text{ m w.e. a}^{-1}$  in the Kunlun mountains. Maurer et al. (2019) found a doubling of the average loss rate during 2000–2016 ( $-0.43 \pm 0.14 \text{ m w.e. a}^{-1}$ ) compared to

设置了格式: 字体: (中文) + 中文正文 (等线)

1976–2000 ( $-0.22 \pm 0.13$  m w.e.  $\text{a}^{-1}$ ), using the KH-9 images and ASTER DEMs. These studies showed that as mentioned above, glacier changes on the TP have obvious marked spatial and temporal heterogeneity, which is probably likely associated with variable glacial response sensitivity to climate change (Yao et al., 2012). Besides, the influence of debris cover, glacial lakes, ice cliffs and glacier morphology on local scales is also included (Brun et al., 2018, 2019; Ke et al., 2020; Maurer et al., 2019).

Detailed, spatially-comprehensive and long-running observations of area and volume change for the WNT are still lacking, however, resulting in there are still many gaps in our knowledge and our understanding of regional glacier behaviour sensitivity, and the interaction of glaciers with climate change and other influencing factors, leading to considerable uncertainty in predicting future glacier area and volume and their runoff yield in this region (Bhattacharya et al., 2021; Immerzeel et al., 2020; Maurer et al., 2019).

The WNT is located in the transition zone between large scale atmospheric circulations, westerlies and Indian summer monsoon. There are an abundance of glaciers and glacial lakes, especially the glacier-fed Nam Co Lake located in the northwest of the WNT, the recent intensified melting of glaciers in the WNT is the main reason for the rising water levels of Nam Co according to relevant studies (Bolch et al., 2010). The number of glacial lakes ( $>0.0036$   $\text{km}^2$ ) in the WNT increased by 56% and their total area increased by 35% between 1976 and 2018 due to the increase in glacial meltwater (Luo et al., 2020). Furthermore, Zhou et al. (2013) revealed the phenomenon of water imbalance in Nam Co Basin based on the measured mass balance data of Zhadang Glacier and other hydrological observation data from 2007 to 2011. In the mostly populated Lhasa Basin located on the TP in the southeast of WNT, Lin et al. (2020) found that water imbalance also existed using the first and second Chinese glacier inventory in 1960 and 2009. Due to logistical limitations of field work, in situ glacier mass balance records are biased towards a few low lying, small glaciers that are difficult to be representative of the entire region (Kääb et al., 2012; Li & Lin, 2017; Yao et al., 2012). The glacier volume in Chinese glacier inventory which was calculated by area-volume formula, and limited observations lead larger uncertainty (Bahr et al., 1997; Bahr et al., 2015). Detailed investigation of the WNT glacier area and mass balance on a longer time scale is absolutely necessary.

So far, investigations of the WNT glacier area have so far focused on the period before 2014 (Bolch et al., 2010; Wu et al., 2016). For glacier mass balance in the WNT, most studies focus on the period after 2000 (Li & Lin, 2017; Neckel et al., 2014; Ren et al., 2020; Zhang & Zhang, 2016). There are limited discussions on glacier changes in the WNT region at local scales before the year of 2000, although Zhou et al. (2018) included this area in his study of glacier mass balance on the TP and its surroundings from the mid-1970s to 2000. Furthermore, the temperature warming rate of the TP is spatio-temporally heterogeneity in recent decades (Duan & Xiao, 2015; Wu et al., 2015). Under a changing river-runoff and the runoff regime is also changing (Lin et al., 2020). The lack of a detailed survey of glacier changes over a long time scale is not conducive a major impediment to water resources management and decision-making (Lutz et al., 2014).

Hence, the key purpose of this study was is therefore to provide an internally-consistent dataset of glacier area and mass change in the WNT range over the past 44 years. We have compiled a complete glacier inventory for the WNT region in the years 1976, 2000, 2014 and 2020 with the Landsat data and KH-9 images to provide information on the general glacier characteristics, and have. Based on KH-9 film, SRTM3.0, and ASTER stereo imagery, we quantified the geodetic glacier

mass balance during from 1976–2000 and 2000–2020, with DEMs derived from KH-9, SRTM3.0, and ASTER. Firstly, We report the glacier area changes and mass balance changes from for periods 1976 to 2000 and from 2000 to 2020 were estimated, and . Secondly, examine the influence of topographic, climatic and glaciological factors glacier terrain on observed glacier area changes and mass balance change was showed, and associated climate drivers in the WNT was discussed.

## 2. Materials and methods

### 2.1 Study area

The WNT range is situated in the southeastern TP (Figure 1), mountain range where has a the mean slope is of 15° and its elevations range is spanning 4150–7125 m, with an average of 4930 m in the whole region. Its 230 km long primary mountain ridge runs in a southwest–northeast direction and extends more than 230 km (Yao et al., 2010) and . The ridge is bounded by the Nam Co basin to the north and the Lhasa River basin to the south. The Nam Co Lake in the Nam Co basin, which is the second largest after Selin Co Lake in the TP and the highest elevation salty lake in the world, is mainly fed by glacier meltwater (Luo et al., 2020; Zhang et al., 2017). The Lhasa River basin, a major branch of the Yarlung Zangbo River, which forms part of the route taken by the warm and humid monsoon airflow into the plateau, is making it warmer and wetter than the Nam Co basin (Luo et al., 2020). The annual air temperature and precipitation in the WNT range from −0.6°C to 2.8°C and 37 mm to 500 mm, respectively (Yu et al., 2013).

Being in a climatic transition zone, The glaciers in this study area is also a transition zone between range from the the maritime-influenced glaciers in of Gangrigabu of (southeast TP), glaciers of subcontinental type (Li & Lin, 2017), and to the continental glaciers in of the Tanggula mountains, where glaciers in the WNT are subcontinental glaciers (Li & Lin, 2017). There are 845 glaciers covering 675.85 km<sup>2</sup> and 15 debris-covered glaciers with a total area of 71.74 km<sup>2</sup>, accounting for 10.61% of the total glacier area in the WNT according to the Randolph Glacier Inventory (RGI-6.0) (RGI Consortium, 2017). Besides Of these, only the small Zhadang Glacier and Gurenhekou Glacier glaciers covering ~ 3 km<sup>2</sup> (red polygon in Figure 1), were performed with have in-situ observation between 2005 and 2010 (Yao et al., 2012), which are. Although the two glaciers cover an area of less than 3 km<sup>2</sup>, mass balance data from field observations can be used available to validate satellite observations.

设置了格式: 上标

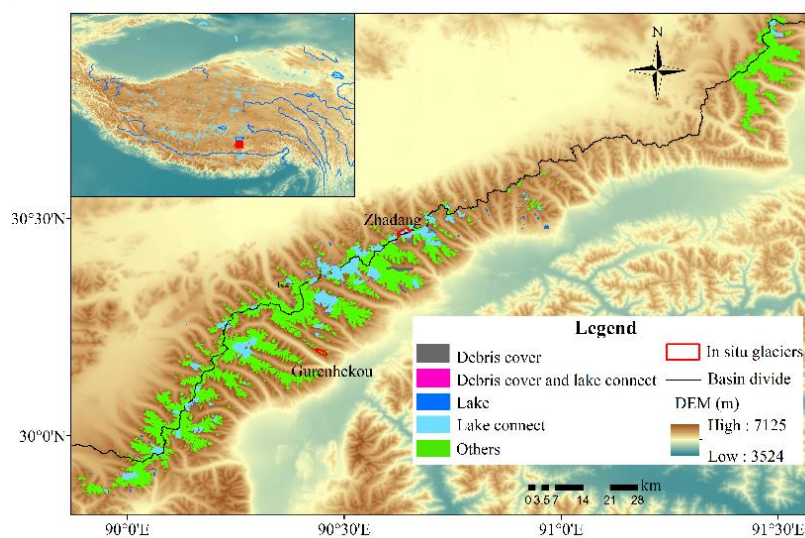


Figure 1 Overview of study area and glacier distribution.

## 2.2 Methods and data

### 2.2.1 Glacier polygons

We identified the glacier boundaries mainly based on the from Landsat MSS/ETM+/OLI scenes from different years (Table 1). The scenes were available from the United States Geological Survey (<http://glovis.usgs.gov/>) and are orthorectified automatically by the USGS using the SRTM3 DEM (level 1T). We selected high-quality images with minimal cloud and snow coverage between June and November were selected for the delineation of glaciers and used a semi-automated approach using the with a TM3/TM5 band ratio ( $2.0 \pm 0.2$ ) was applied to produce glacier outlines. This method is widely used and mostly appropriate for glacier mapping in larger study areas (Guo et al., 2015; Ye et al., 2017). In addition, we used a  $3 \times 3$  median filter to eliminate isolated pixels that are isolated usually and therefore probably misclassified pixels due to rock debris or boulders on the glacier (Bolch et al., 2010). Besides, we manually checked and edited the glacier outlines, including the debris-covered glaciers, with glacier height-changing maps and a coherence map formed by Sentinel-1 images observed on 2016-08-05 and 2016-08-29, to help distinguish debris-covered ice from ice-free areas. Finally, referring to the second glacier inventory, we assigned contiguous ice masses were divided into their drainage basins in order to obtain a glacier inventory.

Table 1. Datasets used to delineate glacier outline for the WNT (1976-2020)

Data	Satellite and sensor	Path/Row	Spatial Resolution (m)	Suitability of scene	Utilisation
1976/01/07	Hexagon KH-9		8	Seasonal snow in the northeast	Glacier inventory in 1976 for whole study area
1976/12/17	Landsat MSS	148/39	30	Little seasonal snow in the northeast	Glacier inventory in 1976 for whole study area except for a
1977/03/17	Landsat MSS	149/39	30	Some clouds	Additional information for glacier of 1976
2000/11/01	Landsat ETM+	138/39	30	Seasonal snow in the northeast	Glacier inventory in 2000 for whole study area

批注 [HP-B4]: Add labels for the Nam Co and Lhasa basins.

2000/11/17	Landsat ETM+	138/39	30	Seasonal snow in the northeast	Glacier inventory in 2000 for whole study area
2001/02/05	Landsat ETM+	138/39	30		Additional information for glacier of 2000
2014/08/12	Landsat OLI	38/39	30	Little clouds	Glacier inventory in 2014 for whole study area
2014/10/15	Landsat ETM+	138/39	30	Some stripes	Additional information for glacier of 2014
2014/06/17	Landsat ETM+	138/39	30	Some stripes	Additional information for glacier of 2014
2016/08/05	Sentinel-1				Check debris glacier
2016/08/29	Sentinel-1				Check debris glacier
2020/09/29	Landsat OLI	138/39	30	Little clouds	Glacier inventory in 2000 for whole study area
2020/10/15	Landsat OLI	138/39	30		Glacier inventory in 2000 for whole study area
2020/09/18	Sentinel-2		20	Little clouds	Additional information for north-eastern glacier of 2020
2020/10/16	Sentinel-2		20		Additional information for south-western glacier of 2020

### 2.2.2 Glacier elevation change

We used the KH-9 images and the SRTM DEM (version 3) to estimate glacial elevation changes for the period 1976 to 2000, and the ASTER DEMs to assess glacier elevation changes for the period 2000-2020.

#### 2.2.2.1 DEM data

The KH-9 images were obtained by a military spy satellite (the KH-9 Hexagon mission) operated from 1971 to 1986, with a ground resolution ranging from 6 to 9 m (Surazakov & Aizen, 2010), and images were declassified by the United States Geological Survey (USGS) in 2002. We downloaded images from 1976-01-07 via the Earth Explorer user interface (<https://earthexplorer.usgs.gov>) and the KH-9 image of 1976-01-07 was acquired. We adopted the Hexagon Imagery Automated Pipeline methodology to extract-generate a digital elevation model. This methodology is coded in MATLAB and uses the OpenCV library for Oriented FAST and Rotated BRIEF (ORB) feature matching, uncalibrated stereo rectification, and semi-global block matching algorithms (Maurer & Rupper, 2015).

The SRTM mission carried out in February 2000 produced two types of DEM datasets, the C-band DEM with a coverage range of 60°N ~ 60°S and the X-band DEM with a smaller coverage. We used the version 3 of the C-band SRTM DEM (<https://earthexplorer.usgs.gov/>) at 1-arc-second resolution (about 30 m) in our primary processing and masked out areas with gaps in the unfilled where the DEM were not truly obtained in 2000 referred to the SRTM3 version 2.1 DEM at 3-arc resolution (about 90 m) without gap-filling.

The ASTER instrument was launched on the Terra satellite as part of a cooperative effort between NASA and Japan's Ministry of Economy Trade and Industry in December 1999 and a The Data1.13a.demz geotiff product with a spatial resolution of 30 m was used and a single DEM covers approximately 3600 km<sup>2</sup>. We downloaded 333 'Data1.13a.demz' ASTER DEMs at 30 m resolution in geotiff format, which with cloud coverage are of less than 40%, were downloaded from the METI AIST Data Archive System (MADAS) satellite data retrieval system (<https://gbank.gsj.jp/madas>). After cloud and outlier removal, we fitted a linear regression through the time series of co-registered ASTER DEMs to estimate the rate of elevation change for each 30-m pixel. Detailed cloud removal and linear fitting procedures refer to the literature (Maurer et al.,

设置了格式: 字体: 五号

2019) to estimate the rate of elevation change for each 30-m pixel.

#### 2.2.2.2. Co-registration and bias correction of DEMs

All DEMs (including ASTER) DEMs were co-registered to the SRTM master DEM using a standard elevation–aspect optimization procedure (Nuth & Kääb, 2011). Then, the elevation correlation deviation of all the DEMs was corrected by the a third-order polynomial. In addition, we used the a 2km square-buffer zone of around the union of glacier boundaries in two phases to define stable (stable–unchanging) terrain for DEMs alignment, and elevation deviation–bias correction and uncertainty calculation. Figure. 2a showed the coverage of the KH image and the number of valid ASTER DEMs grids after removal of clouds and outliers removal in the square buffer. The glacier area covered by the dataset from 1976 to 2000 and from 2000 to 2020 accounted for 70.85% and 81.94% of the total glacier area, respectively (shown in Figure. 2b,c). We used only the area common to both of these datasets to measure elevation change between the 1976–2000 and 2000–2020 periods. In particular, the extent of glacier elevation changes from 2000 to 2020 used for comparison with 1976–2000 was the same as that from 1976 to 2000. After correction for alignment correction and elevation–related deviation corrections, elevation changes of stable terrain (masked glaciers and lakes in square buffer zone) had no change trend with elevation, slope and aspect, as shown in Figure. 3.

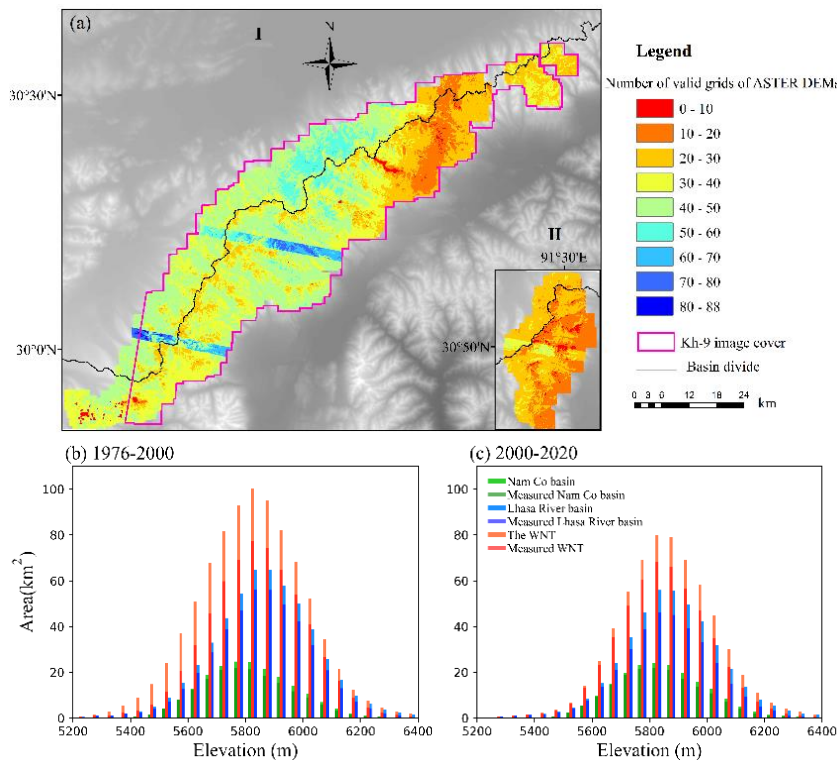


Figure 2 (a) Coverage of KH image and the number of valid ASTER DEMs grids after cloud and outliers removal in the square-buffered area shown. Label I represents the SW section and label II represent the NE section of

带格式的: 缩进: 首行缩进: 0 字符



the WNT ([inset, same map on the same scale](#)). (b) and (c) showed the total area of glaciers and glacier area covered by the datasets respectively during 1976-2000 and 2000-2020.

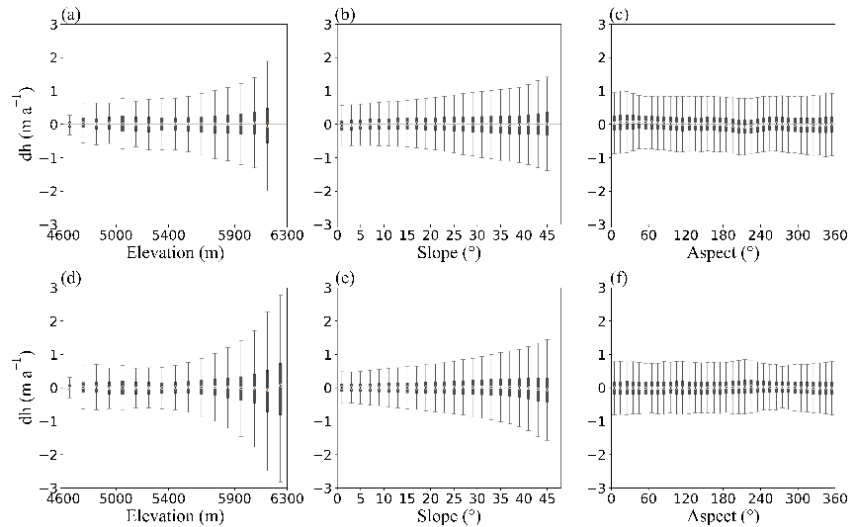


Figure 3 (a), (b) and (c) After alignment correction and elevation related deviation correction, elevation change of stable terrain varies with elevation, slope and aspect during 1976-2000; (d), (e) and (f) showed that of 2000-2020.

#### 2.2.2.3. SRTM $P_{\text{penetration-depth}}$ correction

Over the WNT, [as estimated by Li & Lin \(2017\)](#), the average penetration depth of C-band SRTM is  $1.67 \pm 0.53$  m, [calculated using by using the X-band SRTM DEM as the reference \(Li & Lin, 2017\)](#). Linear regression between the glacier elevation and penetration showed that the penetration depth [is varies from 1.29 m and to 2 m at the altitudes of 5550 m and 6250m respectively \(Li & Lin, 2017\)](#). [We used this more accurate, linear altitude-dependent correction. The method is a more accurate penetration estimation method \(Ke et al., 2020\) and the result is quite similar to compared to several other study regions on the TP \(Gardelle et al., 2013; Kääb et al., 2012\). Therefore, the linear penetration estimation of Li & Lin \(2017\) is adopted in this study.](#)

#### 2.2.2.4 Glacier mass change

Estimation of average glacier thickness changes based on elevation difference maps [includes involves noise filtering and glacier-hypsometry-weighted averages in an approach which are widely employed in to calculate estimating regional glacier mass balance \(MB\) due to where glacier thinning being is highly dependent on altitude. Firstly, we subjected the thickness-change maps were subjected to outlier removal using a thresholds of 150 m threshold which has been used widely used in previously literatures \(e.g., Gardelle et al., 2013; Lin et al., 2017; Neckel et al., 2017\), then. Then thickness change maps were masked where slopes was larger than  \$> 40^\circ\$ , where uncertainties are large \(Figure 3b, c\), before visually inspecting the final thickness change maps were visually inspected. We additionally masked out and any remaining erroneous-anomalous pixels, \(which occurred almost exclusively in low-contrast, snow-covered accumulation zones.\) were manually masked. Finally, we separated thickness changes were separated into 50-m elevation bins by](#)



referring to the SRTM at different spatial scales, i.e., the whole glacierized area, sub-regions, different glacier types and individual glaciers of area  $>2 \text{ km}^2$ . In each altitude bin, we filtered out any height-changed  $dh$  values that differed by more than three standard deviations from the median and ~~were filtered removed~~. Any bins with less than 100 pixels ~~were removed~~. For elevation bins with no observations (mostly over the low- and high- elevation limits), we assumed zero of mean elevation changes ~~were assumed~~. We calculated ~~the~~ the mean glacier thickness changes for the spatial unit/group ( $dh$ ) ~~was calculated~~ as a hypsometric average: ~~as showed in equation (1)~~

$$dh = \sum_{i=1}^n \frac{S_i}{S} \cdot \overline{dh_i} \quad (1)$$

where  $i$  and  $n$  denote the  $i^{\text{th}}$  50-m elevation bin and the number of total bins respectively,  $S_i$  is the glacier area of the  $i^{\text{th}}$  elevation bin,  $S$  is the total glacier area, and  $dh_i$  is the mean  $dh$  in the bin.

We calculated ~~the~~ the final geodetic mass balance ( $B$ ) ~~was calculated by using~~ equation (2).

$$B = dh \times \frac{\rho_{ice}}{\rho_{water}} \quad (2)$$

We translated ~~the~~ glacier thickness changes ~~were translated~~ into mass balance by the ratio of ice column-averaged glacier density, density-to-water density.  ~~$\rho_{ice}$  is the ice density (850  $\text{kg m}^{-3}$ ) and to water density ( $\rho_{water}$  is the water density ( $\sim 1000 \text{ kg m}^{-3}$ ).~~

### 2.2.3 Uncertainty

#### 2.2.3.1 Uncertainty of glacier area

Similar to previous studies (Wu et al., 2016; Ye et al., 2017), we obtained the uncertainty of glacier area ( $\delta_c$ ) ~~was obtained~~ using equation (3)

$$\delta_c = L_c E_{pc} + L_d E_{pd} \quad (3)$$

where  ~~$\delta_c$  is the uncertainty of glacier area~~,  $L_c$  and  $L_d$  represent the lengths of the clean-ice and debris-covered glacier outlines, and  $E_{pc}$  and  $E_{pd}$  denote the positional accuracies. We calculated ~~the~~ the uncertainty in glacier area change ( $\delta_{ac}$ ) by adding combining the area uncertainties; ~~can be calculated~~ using the following equation (4)

$$\delta_{ac} = \sqrt{(\delta_{c1})^2 + (\delta_{c2})^2} \quad (4)$$

Guo et al. (2015) compared glacier outlines derived from Landsat-images with real-time kinematic differential GPS (RTK-DGPS) measurements, and found ~~that an~~ average offsets difference of  $\pm 11 \text{ m}$  and  $\pm 30 \text{ m}$  for the delineation of clean and debris-covered ice. Using a buffer size of  $10 \text{ m}$  ~~was~~ for areas calculated from the Hexagon images (Bolch et al., 2010). ~~Therefore, the our combined~~ uncertainty in glacier area is 3.9%, 5.1%, 5.1% and 5.9% for Landsat images in 1976, 2000, 2014, and 2020, respectively.

#### 2.2.3.2 Uncertainty of glacier thickness change

The ~~errors uncertainty of in~~ surface-elevation changes derived from ASTER DEMs can ~~then~~ be estimated using the mean standard error ( $SE$ ) and mean elevation differences ( $MED$ ) from off-glacier regions.

$$\delta_{dh} = \sqrt{MED^2 + SE^2} \quad (5)$$

批注 [HP-B5]: It is unusual to use the standard deviation along with the median. Standard deviation is usually used with the mean, while the interquartile range is usually used with the median. It does not matter very much in this case so you could leave it in and see if a reviewer complains.

批注 [HP-B6]: Why not correct for the MED bias rather than combine it in the uncertainty? E.g., if the mean difference in stable areas is 3 m, subtract 3 m from the elevation change. This de-biasing then leaves just the SE as the uncertainty.

$$SE = \frac{SD}{\sqrt{N_{eff}}} \quad (6)$$

$$N_{eff} = \frac{N \cdot P}{2D} \quad (7)$$

Where Here,  $MED$  refers to the glacier-hypsometry weighted average of  $dh$  over the off-glacier areas,  $N$  and  $N_{eff}$  represent the total number and independent measurements of pixels respectively,  $SD$  is the standard deviation over off-glacier regions,  $P$  is the DEM spatial resolution (30 m in our study) and  $D$  is the autocorrelation length. We used an autocorrelation length of 500 was employed, which is a conservative value based on semivariogram analysis of mountainous regions in previous studies (Brun et al., 2018; Maurer et al., 2019). In addition We combined, the uncertainty of surface-elevation changes derived from the KH-9 DEM and the SRTM needs to be added to with the penetration error uncertainty, estimated as a value of  $\pm 0.53$  m for penetration error according to (Li & Lin, (2017) was adopted in this study.

We estimated the overall uncertainty in the total glacier mass balance change ( $\delta m$ , in kg) including the uncertainty in the assumed ice/firn/snow density ( $\delta \rho = 60 \text{ kg m}^{-3}$ , which is 7.1% of  $\rho_{ice} = 850 \text{ kg m}^{-3}$ ), errors in glacier area ( $\delta s$ ,  $\text{m}^2$ ) and glacier elevation change ( $\delta e$ , m), was estimated by using equation (8).

$$\delta_m = \sqrt{(S \cdot dh \cdot \delta_\rho)^2 + (\delta_s \cdot dh \cdot \rho_{ice})^2 + (S \cdot \delta_{dh} \cdot \rho_{ice})^2} \quad (8)$$

#### 2.2.4. Lake data

We identified glacier-marginal lakes as those lying within 50 m of a glacier boundary, using lake data for the Lake data from Data on glacial lakes in the western Nyainqentanglha range (1970s-2018) (Luo et al., 2020; http://data.tpd.ac.cn); and glacier data from Referring to Brun et al. (2019).

, we selected the glaciers in contact with lakes (within a 50 m buffer) as lake terminating glaciers.

#### 2.2.5. Meteorological data

There are three meteorological stations adjacent to the NWT, namely the at Bange ( $31^\circ 23' \text{N}$ ,  $90^\circ 01' \text{E}$ ), Lhasa ( $29^\circ 40' \text{N}$ ,  $91^\circ 08' \text{E}$ ), and Damxung ( $30^\circ 29' \text{N}$ ,  $91^\circ 06' \text{E}$ ), distributed adjacent to the WNT. We obtained Air temperature and precipitation data during for 1976-2000 were obtained from the Climatic Data Center, National Meteorological Information Center, of the China Meteorological Administration.

We also obtained Gridded data of precipitation and temperature with spatial resolution of  $0.1^\circ \times 0.1^\circ$  and 3-h time interval during for 1979-2018 are from the China Meteorological Forcing Data set (Yang & He, 2019; http://data.tpd.ac.cn), which has been widely utilized in land process, hydrological modelingmodelling and other studies (Qiao et al., 2021; Wang et al., 2020, 2021). This dataset is made by fusing the conventional meteorological observation of China Meteorological Administration based on the Princeton reanalysis data, GLDAS data, GEWEX-SRB radiation data, and TRMM precipitation data as the background field (He et al., 2020; Yang et al., 2010).

### 3. Results

批注 [HP-B7]: Not 2020?

设置了格式: 字体颜色: 文字 1

带格式的: 正文, 缩进: 首行缩进: 0.74 厘米

### 3.1 Area change

There were 921 glaciers with a total area of 589.17 km<sup>2</sup> in 2020 in the WNT (Figure 4a). Small glaciers dominated the number (those ≤1 km<sup>2</sup> occupy 83.17% of the total number) and ~~occupied~~ also a larger proportion of the area (those ≤1 km<sup>2</sup> occupy 30.42% of the total area). Glaciers ~~with~~ area-larger than 5 km<sup>2</sup> accounted for 21.39% of the total area and only 1.63% of the total number. ~~In addition,~~ gGlaciers were mainly distributed in the eastern-oriented zone with an altitude of 5600-6100m and a slope of 5-40° (Figure 4b,c,d).

~~As can be seen from Figures 4 and 5,~~ gGlaciers in the WNT experienced significant retreat ~~changes~~ from 1976 to 2020 and altitude, slope and aspect all ~~appear to have had obvious~~ influenced ~~on the this~~ retreat (Figures 4 and 5) ~~of glacier area~~. The glacier area decreased by 33.42% ~~from~~ 884.90 km<sup>2</sup> in 1976 to 589.17 km<sup>2</sup> in 2020, with an average annual decrease of -0.76% a<sup>-1</sup>. ~~Figure 5 and Table 2 showed that~~ tThe retreat rate of glacier area in 2000-2020 (1.17% a<sup>-1</sup>) was ~~more than~~ twice as fast ~~as in 1976-2000 (0.54% a<sup>-1</sup>)~~ (Figure 5, Table 2), ~~and the retreat rate in 2000-2020 was more than twice as much as that of 1976-2000. Besides, the r~~Retreat was ~~more significant~~ greatest in the area ~~size-classes~~ of 1-3 km<sup>2</sup> and 3-5 km<sup>2</sup>, and glaciers with significant ~~area~~ retreat were mainly distributed below 6,000 m ~~above sea level~~ altitude. Glaciers ~~in the area of the inside~~ Nam Co basin retreated slightly faster ~~than that of~~ than those outside Nam Co ~~this~~ basin between 2000 and 2020. ~~Moreover, Glacier area reeeded~~ Retreat was extremely sharply particularly ~~rapidly at in the lower~~ altitudes ~~area~~, and ~~the retreat rate~~ decreased with ~~the increas~~ ing of altitude. As for the effect of slope ~~and aspect~~, the glaciers ~~area~~ retreated ~~more rapidly with increasing slope~~ rate between 5° and 40° ~~increased with the increase of slope~~, but the retreat rate decreased ~~with~~ as slope ~~increased~~ between 0°-5° and 40°-60°, where ~~relatively~~ few glaciers ~~are~~ distributed. During both 1976-2000 and 2000-2020, the retreat rate was ~~smallest~~ on the ~~north~~ ern-facing slopes. ~~However, during~~ During 1976-2000, ~~the glacier area shrank~~ retreat was most rapidly ~~on in the south~~ east ~~ern and eastern slope~~ quadrant, while from 2000 to 2020, ~~rapid retreat occurred at similar rates in all aspects other than north and southeast~~ the glacier area decreased most rapidly on the northwestern slopes. But the decreased rate on the northwest slope was slower than that on the southern and eastern slope during 1976-2000. The, i.e., the effect of aspect on glacier area retreat ~~had time heterogeneity~~ varied in space and time.

批注 [HP-B8]: Can you add the uncertainty estimate +/-?

批注 [HP-B9]: Uncertainty estimate +/-?

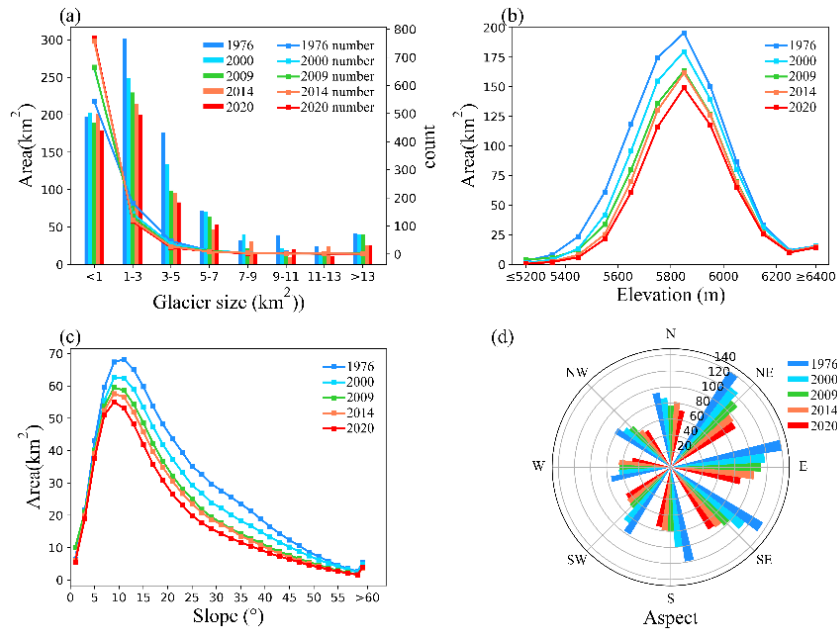
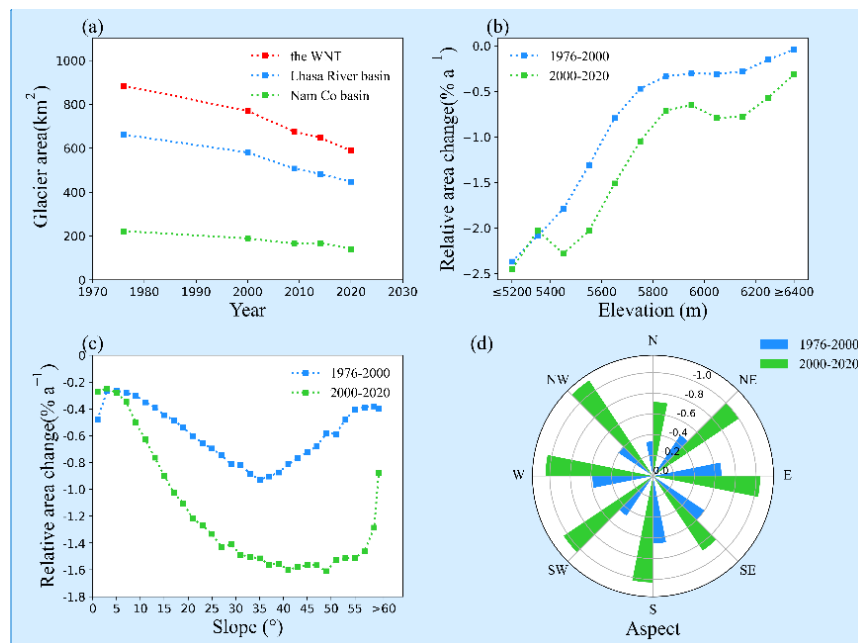


Figure 4 Glacier distribution in the WNT in the year 1976, 2000, 2009, 2014 and 2020. (a) Number and area of glaciers in different size categories. (b) The distribution of glacier area with altitude. (c) The distribution of glacier area with different slope. (d) The distribution of glacier area with different aspects. Data in 2009 came from RGI6.0.



批注 [HP-B10]: Can you add error bars in a,b,c to show whether the change is significant?

Figure 5 Glacier area changes with time (a), elevation (b), slope (c), and aspect (d).

Table 2 Glacier area changes over the WNT from 1976 to 2020

	1976	2000	2020	1976-2000	2000-2020	1976-2020
	Area (km <sup>2</sup> )	Area (km <sup>2</sup> )	Area (km <sup>2</sup> )	△Area (% a <sup>-1</sup> )	△Area (% a <sup>-1</sup> )	△Area (% a <sup>-1</sup> )
The WNT	884.90	770.03	589.17	-0.54	-1.17	-0.76
Lhasa River basin	662.23	580.81	447.93	-0.51	-1.14	-0.74
Nam Co drainage basin	222.58	189.22	141.22	-0.62	-1.27	-0.83

批注 [HP-B11]: Can you add uncertainty columns to this table?

设置了格式: 字体: 8 磅

格式化表格

设置了格式: 字体: 8 磅

设置了格式: 字体: 8 磅, 上标

设置了格式: 字体: 8 磅

设置了格式: 字体: 8 磅

设置了格式: 字体: 8 磅

设置了格式: 字体: 8 磅

### 3.2 Geodetic Mass balance

A map of glacier height changes for the past 44 years, was given are shown in Figure 6. Significant Substantial and near-ubiquitous glacier surface lowering thinning has been observed occurred in the WNT since 1976, with a widespread increase in mass losses tending to increase in the most recent decades. From 1976-2000, Gglaciers experienced a mean thinning elevation rate of  $-0.31 \pm 0.09$  m/year, equivalent to a mean mass loss of  $0.26 \pm 0.08$  m w.e. a<sup>-1</sup> ( $-0.24 \pm 0.08$  Gt a<sup>-1</sup>) from 1976 to 2000. While betweenFrom 2000 and 2020, the mean thinning elevation rate was  $-0.44 \pm 0.17$  m a<sup>-1</sup>, equivalent to a mean mass loss of  $0.37 \pm 0.15$  m w.e. a<sup>-1</sup> ( $-0.29 \pm 0.12$  Gt a<sup>-1</sup>). Several glacier tongues have suffered severe thinning, exceeding  $-1.5$  m a<sup>-1</sup> from 1976 to 2000, especially several long glaciers without debris-cover on the southwesternsouth-western slope. From 2000 to 2020, the range of glacier tongues exceeding losses of over  $-1.5$  m a<sup>-1</sup> is expandeding, and the glacier loss iwas more significant greater in the northeasternnorth-eastern region of the WNT (see, the dotted rectangular box in Figure 6). Moreover, iIn both 1976-2000 and 2000-2020, the glacier downwastinglowering rate iwas slightly higher inside the Nam Co drainage basin than outside it (Table 3, Figure. 7), though these rates do not differ by more than their combined uncertainties. Glacier elevation change, mass balance and total mass change over the WNT, Lasa River basin and Nam Co drainage basin during 1976-2020 were listed respectively in Table 3.

批注 [HP-B12]: Does this include the uncertainty in the density? It is a bit surprising that this uncertainty is smaller than the 0.09 m thinning uncertainty above.

Table 3 Glacier elevation change, mass balance and total mass change over the WNT from 1976 to 2020

	1976-2000			2000-2020		
	Elevation change (m a <sup>-1</sup> )	Mass Balance (m w.e.a <sup>-1</sup> )	Total mass change (Gt a <sup>-1</sup> )	Elevation change (m a <sup>-1</sup> )	Mass Balance (m w.e.a <sup>-1</sup> )	Total mass change (Gt a <sup>-1</sup> )
The WNT	$-0.31 \pm 0.09$	$-0.26 \pm 0.08$	$-0.24 \pm 0.08$	$-0.44 \pm 0.17$	$-0.37 \pm 0.15$	$-0.29 \pm 0.12$
Lhasa River basin	$-0.25 \pm 0.09$	$-0.25 \pm 0.08$	$-0.21 \pm 0.05$	$-0.40 \pm 0.17$	$-0.34 \pm 0.15$	$-0.26 \pm 0.09$
Nam Co drainage basin	$-0.36 \pm 0.09$	$-0.31 \pm 0.08$	$-0.06 \pm 0.02$	$-0.52 \pm 0.17$	$-0.44 \pm 0.15$	$-0.06 \pm 0.03$

批注 [HP-B13]: Can you add a 1976-2020 column like in Table 2?

设置了格式: 字体: 8 磅

格式化表格

设置了格式: 字体: 8 磅

设置了格式: 字体: 8 磅

设置了格式: 字体: 8 磅

设置了格式: 字体: 8 磅

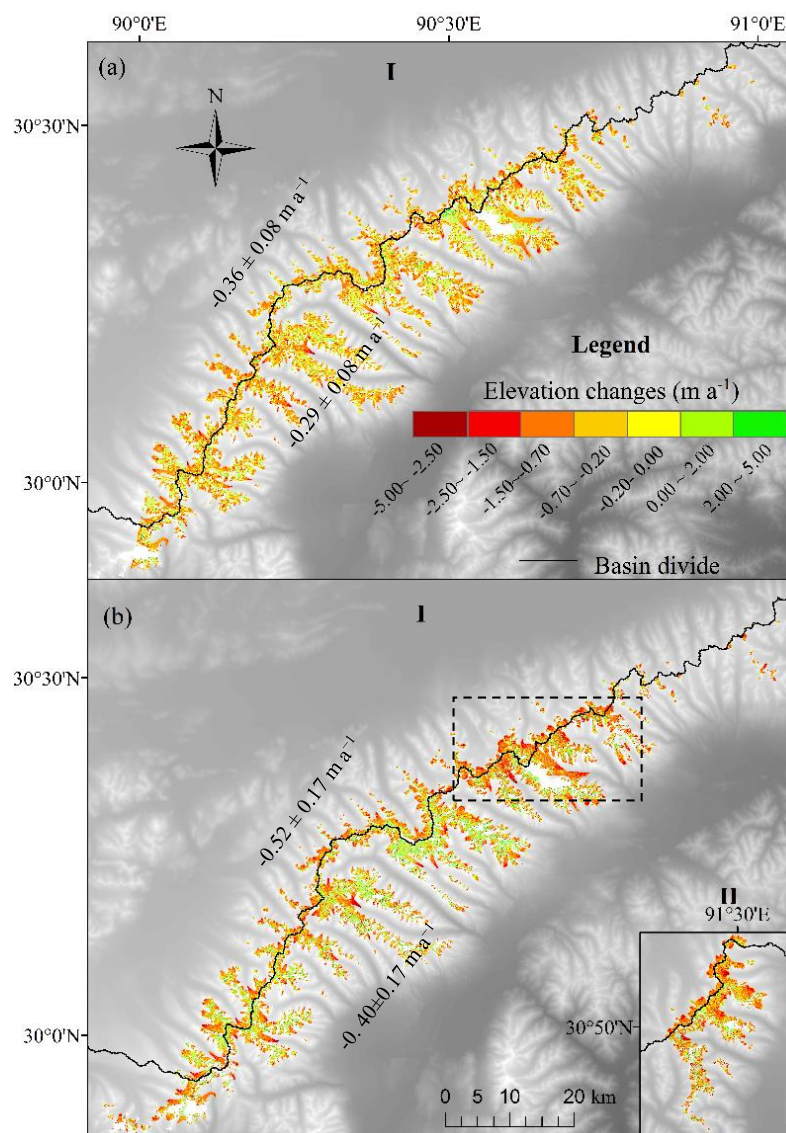


Figure 6 Mean annual glacier surface elevation changes in the WNT from 1976 to 2000 (a), from 2000 to 2020 (b). **Label I** represents the SW section and **Label II** represents the NE section of the WNT (on the same map scale). The dashed box shows an area of the central WNT referred to in the text.

**批注 [HP-B14]:** The light-green  $+0.00-2.00 \text{ m per year}$  class covers a very wide possible range of thickening. Can you add more, smaller thickening classes like those for thinning, at least for the smaller numbers? e.g.,  $+0.00-0.20$ ,  $+0.20-0.70$ .

Figure b looks a lot greener (more thickening) than figure a – is this right?

**批注 [HP-B15]:** Here and other figures – the journal will probably require a different colour scale that does not include both red and green because colour-blind people cannot see a difference. Red-blue works well.

**批注 [HP-B16]:** It would be interesting to see a map of the apparent height change on the stable areas in the buffer around the glaciers, to see what the spatial pattern of the errors is.

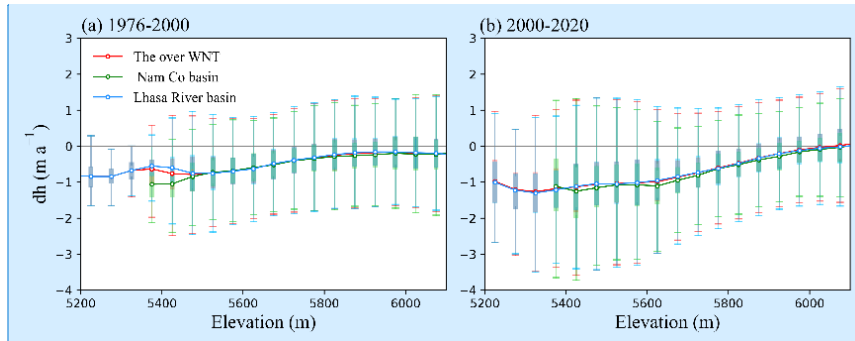


Figure 7 Glacier elevation changes in relation to elevation (m a.s.l.) in the whole WNT, inside Nam Co drainage basin and outside Nam Co drainage basin from 1976 to 2000 (a), from 2000 to 2020 (b). The dots represent the mean elevation change in each 50-m elevation bin.

Besides, we calculated the mass balance of For glaciers with an area of more than 2 km<sup>2</sup>— we and found that the spatial distribution of glacial mass change was basically broadly similar for the periods 1976-2000 and 2000-2020 (Figure 8), with high loss rates. The negative balance was significant in the northeast, followed by the southwest, and moderate in the middle. Mass loss was substantially more intense in 2000-2020, however. In this period, Only a very small number of glaciers with area of 2-5 km<sup>2</sup> were in a state of positive balance, as shown in (Figure 5, by blue dots) at different depths during 2000-2020. and Between 2000 and 2020, the mass balance loss of from some glaciers in the northeast was less than exceeded -0.6 m w.e. year<sup>-1</sup>, and it was not difficult to see from Figure 8 that glacier melting was more intense in 2000-2020.

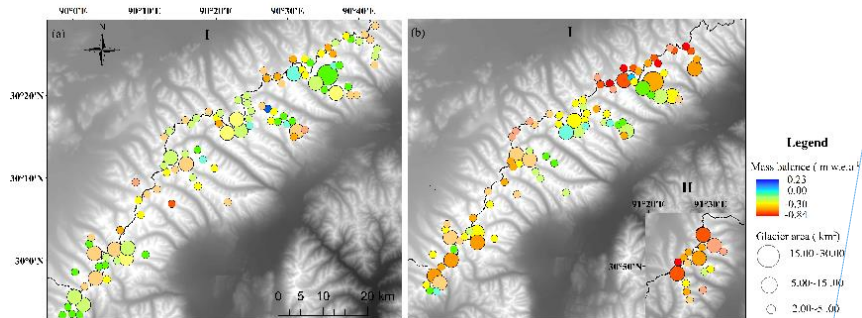


Figure 8 The distribution of glacier-wide mass balance for individual glaciers (> 2 km<sup>2</sup>) in the WNT from 1976 to 2000 (a), from 2000 to 2020 (b), and Label I represents the SW section and II represent the NE section of the WNT (on the on the same map scale).

Finally, the changes of glacier elevation with change as a function of elevation, slope and aspect were shown in Figure 9. Elevation is inversely correlated with had a strong control effect on glacier thickness change, while slope and aspect appear to have had a weak control effect on relationship with glacier thickness change. In both 1976-2000 and 2000-2020, in the low elevation region, the glacier's elevation change rate was the largest at lower altitudes, and the

批注 [HP-B17]: What do the thicker error bars (of about +/- 0.5 m/a) represent?

批注 [HP-B18]: Can you change the colour scale so that it is symmetrical around zero - so all blueish colours are thickening and all reddish colours are thinning, between e.g., +0.81 to -0.81 m w.e./yr? This will make it easier to compare the magnitudes of thickening versus thinning.



melting rate gradually decreased with the increasing of altitude. Similarly, the thinning rate of glacier thickness also exhibited a weak inverse relationship with slope, becoming somewhat stronger in the 2000-2020 period. The thinning rate decreased with the increase of slope except that the elevation change rate between 0-8 degrees increased slowly with the increase of slope during 1976-2000. For the impact of aspect, the glacier thickness change thinning for 1976-2000 rate was the largest most rapid in the south-west and north-west quadrants, but by 2000-2016, high thinning rates were affecting all aspects, i.e., the northwestern slope and the ablation rate is smaller on the eastern and the northern slopes during both 1976-2000 and 2000-2020. However, the thickness thinning rate on the northern, northeastern and eastern slopes, which was small during 1976-2000, increased significantly during 2000-2020, while the thickness thinning rate on the southern, southwestern and western slopes with large thickness thinning rate during 1976-2000 did not increase significantly during 2000-2020. The effect of slope-direction aspect on the ablation thinning rates also of thickness was also time heterogeneous varied through time.

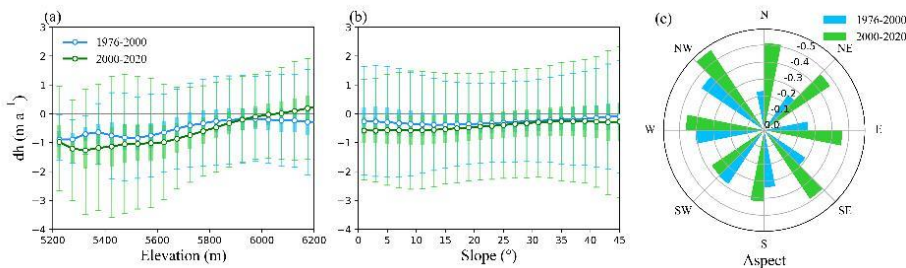


Figure 9 Glacier elevation changes in relation to elevation (m a.s.l) in the WNT from 1976 to 2000 (a), and from 2000 to 2020 (b). Red boxplots were statistically drawn in 50-m elevation bins. Bars in light blue and dark blue represent the total area of glaciers and the measured glacierized area respectively. Glacier elevation changes in relation to slope and aspect in the WNT (c, d). The dots in figure (eb) represent the mean elevation change in each 1-° slope bin and the bars in figure (c) represent the mean elevation change in each 45-° aspect bin.

批注 [HP-B19]: Not red.

### 3.3 The effect of debris-cover and glacial-lake-connection ice-marginal lakes on glacier mass changes

In the our WNT study area, there were are five debris-covered glaciers, covering and its area was 55.42 km<sup>2</sup> in 1976 and 51.49 km<sup>2</sup> in 2000. Lake-terminating glaciers occupied a similar proportion, with area of 70.29 km<sup>2</sup> in 1976, and 49.60 km<sup>2</sup> in 2000. Only one glacier was both covered by debris and terminated with in a pro-glacial lake.

The detailed information of area and mass balance of different types glaciers was summarized in Table 4.

Figure 10 and table 4 showed that the melting thinning rate of different types of glaciers varied greatly (Figure 10, Table 4). During 1976-2000, the lake-terminating glaciers thinned more significantly rapidly, followed by the regular glaciers and the debris-covered lake-terminating glacier, and the debris-covered glacier terminated in proglacial lake which thinned slower in the most elevation bins. However, from 2000 to 2020, the ablation rate of debris-covered glaciers was slightly lower than that of regular glaciers at low altitude, but it was gradually progressively greater than that of regular glaciers as the at higher altitudes, leading to a slightly more negative total mass balance. increases and the mass balance of debris covered glaciers was slightly negative than that of regular

设置了格式: 字体: (默认) Times New Roman

批注 [HP-B20]: Can you show the area uncertainties here?

带格式的: 缩进: 首行缩进: 0 字符

glaciers. Besides, the rapid melting/thinning of lake-terminating glaciers was more significant greater than that of regular glacier during 2000-2020. These findings indicate that debris-cover in the WNT suppressed glacier thinning to some extent and enabled the debris-covered ice to survive at much lower elevations than adjacent clean ice glaciers. In contrast, a glacial lake at the end of a glacier accelerated its retreat and this feature was more pronounced at lower elevations.

Table 4 Statistics of area, quantity and mass balance of different types of glaciers

Glacier type	1976-2000			2000-2020		
	Area (km <sup>2</sup> )	Number	Mass Balance (m w.e.a <sup>-1</sup> )	Area (km <sup>2</sup> )	Number	Mass Balance (m w.e.a <sup>-1</sup> )
Lake terminating	70.29	46	-0.36 ± 0.08	49.60	34	-0.56 ± 0.12
Debris cover	55.42	5	-0.20 ± 0.08	51.59	5	-0.44 ± 0.12
Debris cover and lake terminating	4.06	1	-0.18 ± 0.08	6.05	1	-0.34 ± 0.12
Regular	615.29	617	-0.30 ± 0.08	554.64	692	-0.42 ± 0.12

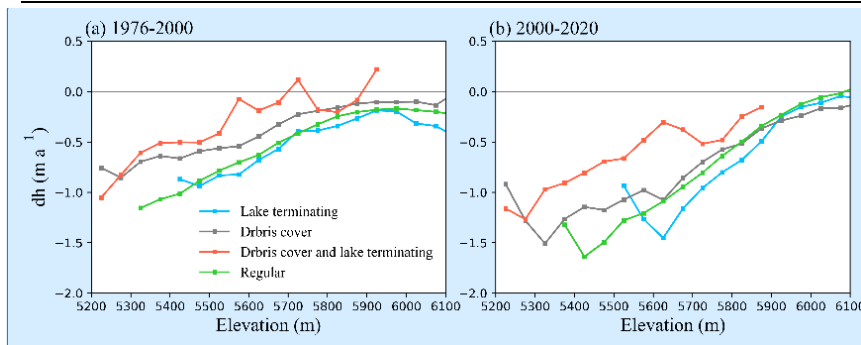


Figure 10 Rate of glacier elevation change with elevation of different type glaciers during 1976-2000 (a), during 2000-2020 (b). Plots represent the mediums of glacier elevation change in each 50-m elevation bin.

## 4. Discussion

### 4.1 Glacier area change

Based on space-borne imagery, we found that glacier area in the west Nyainqentanglha Range (WNT) has retreated/changed by -13.0% from 1976 to 2000 and -23.5% from 2000 to 2020. The comparison between our study and previous studies was/is shown in Tables 5 and 6. Previous glacier change studies found a glacier area decrease by -15.4% inside the Nam Co basin (Wu & Zhu, 2008), and Frauenfelder & Kääb (2009) found an area decrease of -19.8% for the southwest of WNT from 1970 to 2000. While Shangguan et al. (2008) showed an area decrease of -5.7% over the WNT and Bolch et al. (2010b) showed an area decrease of -6.8 ± 3.1% during the similar period. One explanation for the differences between studies may have arisen from could be that the georeferencing errors in the areas in for 1970 used by in research of Shangguan et al. (2008) and Wu & Zhu (2008) which came from the Chinese Glacier Inventory (CGI) based on the Chinese topographic maps, and there are errors in georeferencing in CGI found by (Frauenfelder and Kääb, 2009). Although obvious errors in the CGI was/were omitted in their change analysis, the remaining glaciers was/were not corrected (Frauenfelder & Kääb, 2009). Another explanation for the discrepancies may also have arisen y might be from the differences in the methods used to

批注 [HP-B21]: See also my comment for Table 4 about scaling the uncertainties according to the sample size.

It is best to focus on the large changes that can be described as significant, i.e., those where the means differ by more than the sum of their uncertainties. With the uncertainties you have at present, the significant differences here are between e.g., for 1976-2000, 'lake terminating' compared to 'debris covered' and 'debris-covered and lake terminating'. As there is only one 'debris-covered and lake-terminating' covering 4 km<sup>2</sup>, its mean is likely to be more uncertain than the mean for the much larger (615 km<sup>2</sup>) 'regular' class.

With the current uncertainties, there are also significant differences between e.g., 'lake terminating' and 'debris covered' for 1976-2000 compared to 2000-2020. You could word non-significant changes something like "There are large apparent increases in mass loss between these two periods for regular glaciers and the debris-covered, lake-terminating glacier, though the change in their mean loss rates does not exceed their combined uncertainties".

Alternatively, another way to identify significant changes would be to compare the total height change from 1976-2020 for the different glacier types, rather than for the two periods separately. The difference in their height changes over this longer 44-year period might be so big compared to the

批注 [HP-B22]: I think the uncertainties in the means in Table 3 and 4 need to be scaled according to the sample size (i.e., the number of on-glacier pixels in each class), rather than being constant (0.08 or 0.12).

I think you can calculate this scaled uncertainty as =  $\text{SQRT}((\text{SD}^2/n) + \delta m^2)$

Here, SD is the standard deviation of the mean mass change from all of the pixels in that class, and n is the number of pixels.

批注 [HP-B23]: Adding error bars would help reveal the most significant changes here. It would also be good to make the lines more distinct (e.g., by using dashes etc).

批注 [HP-B24]: This is a different number from the table (-15.8).

interpretation distinguish of glaciers against from seasonal snow, and debris-cover glaciers against from neighbouring moraine or rock slopes from different researchers (Bolch et al., 2010). Comparing to our results to the glacier area changes in 1970-2000 and 1977-2000-2000-2014 from the study of Wu et al. (2016) and in 1977-2000 and 2000-2010-2000-2014 from Wang et al. (2012), our results agree within the uncertainties – a small discrepancy less than 3% was observed over the whole WNT or and the Southwest of WNT respectively. This is equivalent to the uncertainty in glacier area. Besides, taking into account the changes in glacier area, our results are close to those of in 1970-2000 from Wu et al. (2016) and in 2000-2010 from Wang et al. (2012). In addition, the 789.15 km<sup>2</sup> glacier area over-reported for the WNT from by RGI V4.0 (which used applied Landsat images observed obtained on 2001-12-06) agrees with to identify glacier boundary is 789.15 km<sup>2</sup>, and our result (770.03 ± 38 km<sup>2</sup>) was close to the data. Therefore, the result of glacier change over the WNT from this study is reliable.

Table 5 The eComparison of to previous studies and this study on glacier change over the WNT

Time period	Region	Area change (%)	Data	Method	Study
1970-2000	Nam Co Basin	-15.4	Aero-photo topographic map, Landsat ETM+	Manual	Wu & Zhu (2008)
1976-2001	Nam Co Basin	-6.8 ± 3.1	Hexagon KH-9, Corona, Landsat MSS/TM/ETM+	Band ratio and revised manually	Bolch et al. (2010b)
1970-2000	The WNT	-5.7	Aero-photo topographic map, Landsat ETM+, ASTER	Manual	Shangguan et al. (2008)
1970/80-2000	The sSouthwest of WNT near Lhasa	-19.8	LandSat Series, ASTER	Band ratio	Franenfelder & Kaab (2009)
1976-2001	Nam Co Basin	-6.8 ± 3.1	Hexagon KH-9, Corona, Landsat MSS/TM/ETM+	Band ratio and revised manually	Bolch et al. (2010b)
1977-2000	The sSouthwest of WNT	-15.6 ± 3.27	Hexagon KH-9, Landsat	Band ratio and revised manually	Wang et al. (2012)
2000-2010	The WNT	-8.11 ± 3.09	MSS/TM/ETM+	revised manually	Shangguan et al. (2008)
1970-2000	The WNT	-5.7	Aero-photo topographic map, Landsat ETM+, ASTER	Manual	Shangguan et al. (2008)
1970-2000	The WNT	-11.7 ± 3.6	Chinese Topographic Maps, Landsat TM/ETM+	Band ratio and revised manually	Wu et al. 2016
2000-2014	The WNT	-17.8 ± 4.9	Hexagon KH-9, Landsat	Band ratio and revised manually	This paper study
1976-2000	The WNT	-13.0 ± 4.7	MSS/ETM+/OLI	revised manually	
2000-2014		-15.8 ± 6.6			

Table 6 Comparison of glacier area between this study and study of Wu et al. (2016) in specific years

	Glacier Area (km <sup>2</sup> )				
	1970	1976	2000	2014	2020
Wu et al. (2016)	892.61 ± 17.76	-	788.47 ± 25.59	648.23 ± 23.54	-
This paper study	-	884.90 ± 35.35	770.03 ± 37.88	648.55 ± 34.25	589.17 ± 34.68

## 4.2 Mass balance

There are two measured glaciers in the WNT. Field measurements of mass balance are available from small glaciers, namely the Zhadang glacier and Gurenhekou glacier. Zhadang, on the north-western slope of the WNT glacier located on the northwestern slope of the WNT, with in-situ observations between 2005 and 2008, is a small glacier with area of 2.33 km<sup>2</sup> in 2020 for 2005 and 2008, and between 2005 and 2010 for The Gurenhekou, glacier is located on the south-eastern slope of the WNT. The glacier is also a small glacier with area of 1.17 km<sup>2</sup> in 2020 and has in-situ observation data between 2005 and 2010. (Table 7). listed the changes in area and mass balance of

格式化表格

带格式的：左

带格式的：左

带格式的：左

格式化表格

带格式的：左

带格式的：左

格式化表格

带格式的：左

带格式的：左

带格式的：居中

格式化表格

带格式的：左

带格式的：左, 缩进: 首行缩进: 0 字符

带格式的：居中

带格式的：左

带格式的：居中

the two glaciers in this study, and their mass balance derived from in-situ observations. Although the time period of our study is longer, our the results of the mass balance results were are in good agreements similar to these field measurements with that of Zhadang Glacier and Gurenhekou Glacier.

Table 7 The Changes in area (A) and mass balance (B<sub>N</sub>) of Zhadang Glacier and Gurenhekou Glacier in this study, and their mass balance derived from in-situ observations.

Name	1976	2000	2020	1976-2000		2000-2020		1976-2020		in-situ B <sub>N</sub> (m w.e. a <sup>-1</sup> )
	A(km <sup>2</sup> )			ΔA (% a <sup>-1</sup> )	B <sub>N</sub> (m w.e.a <sup>-1</sup> )	ΔA (% a <sup>-1</sup> )	B <sub>N</sub> (m w.e.a <sup>-1</sup> )	ΔA (% a <sup>-1</sup> )	B <sub>N</sub> (m w.e.a <sup>-1</sup> )	(m w.e.a <sup>-1</sup> )
Zhadang	3.74	3.21	2.33	-0.57	-0.16	-1.37	-0.67	-0.84	-0.39	-0.59
Gurenhekou	1.75	1.59	1.17	-0.37	-0.27	-1.32	-0.37	-0.74	-0.31	-0.31

Notation: A and B<sub>N</sub> represents the area and mass balance of glaciers.

Furthermore, previous studies have also reported region-averaged glacier mass balance in of a similar spatial extent to ours, obtained though from DEMs obtained with using various different equipments and satellites sensors (Table 8). However, our results during for 2000-2020 was are more negative than the results from those of Neckel et al. (2014), Li & Lin (2017) and Zhang & Zhang (2017) but agree within the uncertainties over comparable time periods, even though these studies differ in data processing. One reason was that our time scale is longer. Another was the deviations in data processing, such as, glacier mask, penetration correction and data coverage. For comparison, we calculated the Based on ASTRE DEMs, we limited the time scale to change for the 2000-2014 period from ASTER DEMs (Figure 11), and, and the our estimated mass balance in this area was  $(-0.28 \pm 0.12 \text{ m w.e. a}^{-1})$  is very similar to the other studies (Table 8). It is also similar to that of 1976-2000, suggesting that the more strongly negative average for the longer 2000 to 2020 period  $(-0.37 \pm 0.15 \text{ m w.e. a}^{-1})$  is the result of particularly strongly negative mass balance after 2014, although cloud-free ASTER data are insufficient for direct calculation of mass balance from 2014-2020. This interpretation is supported by Glacier thickness changes and data coverage in the WNT during 2000-2014 were shown in Figure 11. From 2000 to 2014, the glacier mass balance of WNT was slightly negative than that of 1976-2000, which was close to the results of from that of Neckel et al. (2014) et al. This means that the glacier mass balance was more negative from 2000 to 2020 mainly because of the intensified glacier melting after 2014, although there was not enough data for direct calculation of mass balance of 2014 to 2000 due to ASTER DEMs being affected by cloud. Moreover, Ren et al. (2020) who also indicted calculated the a mass balance of glaciers in 2013-2020 rate  $(-0.43 \pm 0.06 \text{ m w.e. a}^{-1})$  was twice that as negative as in 2000-2013. Though the difference in rate is within the combined uncertainties for these periods, this apparent acceleration in thinning in WNT. Finally, the study found the thinning rate of  $(-0.26 \pm 0.09 \text{ m w.e. a}^{-1})$  in 1976-2000 to  $(-0.37 \pm 0.15 \text{ m w.e. a}^{-1})$  in 2000-2020 was more faster than that of 1976-2000  $(-0.26 \text{ m w.e. a}^{-1})$  is similar, similar phenomenon to the broader regional pattern of accelerating loss across the Himalayas and Kangri Karpo Mountains (Maurer et al., 2019; Wu et al., 2018, 2019).

Table 8 Mass balance estimates (from geodetic and altimetry studies) over the WNT and comparable sub-regions/catchments.

Time period	Mass balance (m w.e.a <sup>-1</sup> )	Data	Study
1976-2000	$-0.25 \pm 0.15$	KH-9 and SRTM	Zhou et al. (2018)

批注 [HP-B25]: Add uncertainties to this table where possible.

带格式的: 左

2003-2009	$-0.20 \pm 0.29$	ICESat	Neckel et al. (2014)
2000-2013	$-0.22 \pm 0.23$	SRTM and ZiYuan-3 Three-	Ren et al. (2020)
2013-2017	$-0.43 \pm 0.06$	Line-Array stereo images	
2000-2017	$-0.30 \pm 0.19$		
2000-2014	$-0.24 \pm 0.13$	SRTM and TerraSAR-X/TanDEM-X images	Li & Lin (2017)
2000-2014	$-0.26 \pm 0.06$	SRTM and TerraSAR-X/TanDEM-X images	Zhang & Zhang (2017)
1976-2000	$-0.26 \pm 0.09$	KH-9 and SRTM	This <a href="#">paperstudy</a> .
2000-2014	$-0.28 \pm 0.12$	ASTER DEMs	
2000-2020	$-0.37 \pm 0.15$	ASTER DEMs	

带格式的: 左

带格式的: 左

带格式的: 左

带格式的: 左

带格式的: 左

带格式的: 左

带格式的: 左

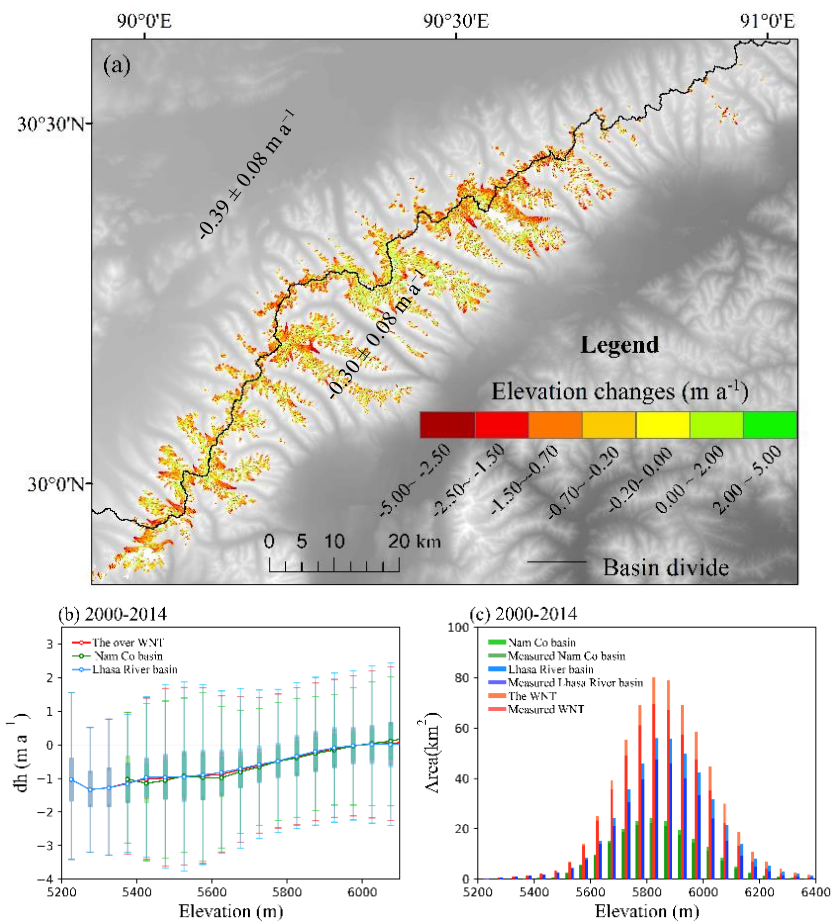


Figure 11 (a) Glacier ~~thickness-elevation~~ change in the WNT during 2000-2014. (b) Glacier elevation changes in relation to elevation in the WNT, inside Nam Co drainage basin and outside Nam Co drainage basin from 2000 to 2014. The dots represent the mean elevation change in each 50-m elevation bin. (c) ~~showed the~~ Total area of glaciers and ~~glacier-that~~ area covered by the datasets during 1976-2000 and 2000-2014.

#### 4.3 The influences of debris-cover and proglacial lakes on glacier mass changes

Debris [can](#) [inhibits](#) or promotes glacial ablation depending on its thickness (Maurer et al., 2016). A shallow layer of debris usually enhance melt rates due to its low surface albedo, while thicker layers could suppress melt rates through the process of thermal insulation (Reid et al., 2012). Besides, another reason for the more negative mass balance of the debris-covered glaciers is that monsoonal summer rainfall might carry heat flux to the underlying ice bodies of debris covered glaciers (Neekel et al., 2017). Several studies indicated that debris covered glaciers are on slower mass loss compared with debris free glaciers (Nicholson & Benn, 2006; Scherler et al., 2011; Vincent et al., 2016). However, large-scale geodetic studies reported that there were no significant differences in the thinning rates between debris-covered and clean glaciers on time scales more than a decade after 2000 (Brun et al., 2019; Ke et al., 2020; Maurer et al., 2019).

Our ~~estimates~~ results (Table 4) suggest that the debris-covered glaciers in our study area thinned more slowly than the regular, debris-free glaciers in the 1976-2000 period, though the difference is not statistically significant and the small sample size (5) of the debris-covered glaciers compared to regular glaciers (>600) limits our ability to compare these classes. In the 2000-2020 period, the thinning rate of the debris-covered glaciers increased significantly, to double its previous rate, though it remains [indistinguishable from the thinning rate for regular glaciers at that time](#). Several previous studies indicated that [on the glacier-scale, debris-covered glaciers thin more slowly than are on slower mass loss compared with debris-free glaciers](#) (Nicholson & Benn, 2006; Scherler et al., 2011; Vincent et al., 2016). However, large-scale geodetic studies reported that [there were no significant differences in the thinning rates between debris-covered and clean glaciers on time scales more than a decade after 2000](#) (Brun et al., 2019; Ke et al., 2020; Maurer et al., 2019), a finding that is supported by this study.

[reported that the melting rate of debris-covered glacier was significantly slower than regular glaciers during 1976-2000, but between 2000 and 2020, the melting rate of debris-covered glaciers was slightly larger than that of regular glaciers. Our result during 2000-2020 was in line with geodetic studies.](#) Banerjee (2017) proposed a theory that the thinning rate of a debris-covered glacier is initially slower than that of a similar clean glacier at the early stage of warming but subsequently matches and then overtakes the counterpart. [BesidesIn this theory, the time required for melting rates to cross between a debris-covered glacier and debris-free glacier seems to be controlled by the rate of warming, and there is little difference between the thinning rates of the two glaciers at a-very low rates of warming](#) (Banerjee, 2017). [The larger difference in the 1976-2000 mean melt rates of the regular versus debris-covered glaciers in our study provides some support for this theory, but a larger sample with lower uncertainty is needed to verify this.](#)

Glaciers with proglacial lakes can experience relatively high mass loss through calving and thermal undercutting (Maurer et al., 2016; Thompson et al., 2012) and the expansion of such lakes can cause dynamic thinning to propagate upglacier (Ke et al., 2020). [is means that the slightly more negative mass balance of debris covered glaciers in the WNT during 2000-2020 indicates an advanced stage of glacier evolution.](#)

Glaciers terminating in proglacial lakes in [thoure](#) study area [have had the highest mean rates of thinning of all of the classes in both time periods...](#)

[more negative mass balances compared to both types of land-terminating glaciers \(both regular and debris covered\) during 2000-2020.](#)

批注 [HP-B26]: We should revisit these sections on differences between glacier types and topographic settings once the uncertainties in Table 4 have been updated to reflect their different sample sizes. This will give a better idea of which changes are significant.

设置了格式: 非突出显示

设置了格式: 非突出显示

设置了格式: 非突出显示

设置了格式: 非突出显示

设置了格式: 非突出显示

设置了格式: 非突出显示

设置了格式: 非突出显示

设置了格式: 非突出显示

设置了格式: 非突出显示

设置了格式: 非突出显示

设置了格式: 非突出显示

设置了格式: 非突出显示

设置了格式: 非突出显示

设置了格式: 非突出显示

设置了格式: 非突出显示

设置了格式: 非突出显示

设置了格式: 非突出显示

设置了格式: 图案: 清除 (黄色), 非突出显示

设置了格式: 非突出显示

设置了格式: 非突出显示

设置了格式: 非突出显示

设置了格式: 非突出显示

设置了格式: 非突出显示

设置了格式: 非突出显示

设置了格式: 非突出显示

设置了格式: 非突出显示

设置了格式: 非突出显示

设置了格式: 非突出显示

设置了格式: 非突出显示

设置了格式: 非突出显示

设置了格式: 非突出显示

设置了格式: 非突出显示

设置了格式: 非突出显示

设置了格式: 非突出显示

设置了格式: 非突出显示

设置了格式: 非突出显示

设置了格式: 非突出显示

批注 [HP-B27]: To be revisited with updated uncertainties.



Glaciers with proglacial lakes usually experienced accelerated mass loss through calving and thermal undercutting processes along with lake expansion (Maurer et al., 2016; Thompson et al., 2012). Moreover, the downward movement of glaciers can transport ice to areas of greatest melting at lower altitude (Ke et al., 2020). The mutually reinforcing effect has great influence on lake outburst flood hazard and water resource management, especially for glaciers terminating in flat valleys where glacial lakes tend to form (Maurer et al., 2016).

#### 4.4 Topographic and climatic drivers-controls of varying glacier mass loss

If climate is the driving force behind the glacier change, the glacier topographical parameters are the controlling factors which modulate these changes (Pandey et al., 2017). Furthermore, the controlling factors of glacier glacier thickness change and glacier area change are complicated, however (Ke et al., 2020), with. In addition, al to topographic factors, they are also related to many other factors, such as climatic conditions including localised climate, glacier thickness, morphology, the presence of proglacial/supraglacial lakes and debris cover, and latitude, and longitude and so on (Brun et al., 2018, 2019; Maurer et al., 2019).

We found that Both glacier area retreat rate (Figure 5b) and thickness thinning rate (Figures 7 and 9) generally decreased with the increase of altitude, which was showed in several studies agreeing with previous studies (Li & Lin, 2017; Wu et al., 2016; Ye et al., 2017; Zhou et al., 2019). However, the effect of slope and aspect on glacier thickness has been rarely studied. We found that in the slope range of 8-40°, where the glaciers were mainly distributed, the rate of area change retreat glacier area increased with the increase of slope (Figure 5c), but the glacier thickness change thinning rate decreased with the increase of slope (Figure 9b). This may reflect the preferential loss (retreat) of relatively thin ice on steeper slopes, even where thinning rates were not exceptional. The effect relationship between aspect on and both glacier area retreat shrinkage and thickness thinning was inconsistent and heterogeneous varied in time (Figures 5d and 9c).

In the WNT, Wu et al. (2016) also showed that glacier area decreased rate increased with the increase of slope. However, the effect of slope and aspect on glacier thickness has been rarely studied. We speculated that glaciers that retreated more quickly generally were thinner, and their thinning rate was smaller. Besides, the glaciers with higher thickness thinning rate become thinner gradually with time, and the thickness thinning rate decreased while the area thinning rate increased. Furthermore, the controlling factors of glacier thickness change and glacier area change are complicated (Ke et al., 2020). In addition to topographic factors, they are also related to many other factors, such as climatic conditions, glacier thickness, morphology, proglacial/supraglacial lakes and debris cover, latitude, longitude and so on (Brun et al., 2018, 2019; Maurer et al., 2019).

The mean glacier mass balance thinning and area change estimates showed slightly consistently higher mean differences rates of thinning and retreat between in the Nam Co drainage basin and than the Lhasa River basin (Tables 2 and 3), in agreement with Bolch et al. (2010) and Li & Lin (2017), and also reported slightly higher glacier melting in the Nam Co drainage basin. Besides, the glaciers in the middle-central of WNT showed particularly strong significant melting from 2000 to 2020. While the glacial distribution mass balance pattern of on the TP broadly follows the regional atmospheric circulation pattern (Yao et al., 2012). However, the variability in glacier mass loss within regions cannot always be fully explained by the varying changes in precipitation and temperature changes on this scale (Wu et al., 2018).

The temperature record from three nearby WNT weather stations showed a consistent warming trend with a mean rate of 0.046 °C a<sup>-1</sup> and the precipitation record showed a slightly

设置了格式: 字体: (默认) Times New Roman

设置了格式: 非突出显示

设置了格式: 字体: (默认) Times New Roman

设置了格式: 非突出显示

带格式的: 图案: 清除 (背景 1)

设置了格式: 非突出显示

设置了格式: 非突出显示

设置了格式: 非突出显示

设置了格式: 非突出显示

设置了格式: 非突出显示

设置了格式: 非突出显示

设置了格式: 非突出显示

设置了格式: 非突出显示

设置了格式: 非突出显示

设置了格式: 非突出显示

设置了格式: 非突出显示

设置了格式: 非突出显示

设置了格式: 非突出显示

设置了格式: 非突出显示

设置了格式: 非突出显示

设置了格式: 非突出显示

设置了格式: 非突出显示

设置了格式: 非突出显示

设置了格式: 非突出显示

设置了格式: 非突出显示

设置了格式: 非突出显示

设置了格式: 非突出显示

设置了格式: 非突出显示

设置了格式: 非突出显示

带格式的: 首行缩进: 0 字符

设置了格式: 非突出显示

设置了格式: 非突出显示

设置了格式: 非突出显示

设置了格式: 非突出显示

设置了格式: 非突出显示

设置了格式: 非突出显示

设置了格式: 非突出显示

设置了格式: 非突出显示

设置了格式: 非突出显示

设置了格式: 非突出显示

设置了格式: 非突出显示

设置了格式: 非突出显示

设置了格式: 非突出显示

设置了格式: 非突出显示

设置了格式: 非突出显示

设置了格式: 非突出显示

设置了格式: 非突出显示

设置了格式: 非突出显示

设置了格式: 非突出显示

设置了格式: 非突出显示

设置了格式: 非突出显示

设置了格式: 非突出显示

设置了格式: 非突出显示

设置了格式: 非突出显示

设置了格式: 非突出显示

批注 [HP-B28]: Can you also show the trend in summer temperature (e.g., the 6 months from April-September), as this is more relevant to melt rates than the annual temperatures.



wetting trend between 1976 and 2020 (Figures 12). The gridded data showed that the temperature in the study area increased more during 2000–2018 than during 1979–2000 (Figures 13), and that precipitation increased during 1979–2000 and decreased during 2000–2018. This corresponds to the temporal heterogeneity pattern of glacier change (glacier loss during 2000–2020 was greater than that during 1976–2000). Furthermore, and the significant warming from 2014 to 2018 (red area in Figure 13) corresponded to a geographically to the significant substantial central-WNT thinning of the glacier highlighted in the dashed rectangular box shown in Figure. 6. Precipitation also increased significantly substantially in the region from 2014 to 2018, and Relevant studies (Li et al., 2020; Oerlemans & Fortuin, 1992) showed that glacier melting was can be extremely particularly intense under combined warm and wet conditions (Li et al., 2020; Oerlemans & Fortuin, 1992).

The Temperature and precipitation data from 2014 to 2018 described above offer a compelling explanation for the main temporal and spatial variations in glacier change in the WNT, particularly the high rates of thinning from 2014–2018, though they do not directly explain why the Nam Co glaciers thinned more rapidly than elsewhere. provided lateral evidence of the dramatic thinning of glacier thickness after 2014, which we indirectly estimated. In a word, the changes of temperature and precipitation could explain the temporal heterogeneity and some spatial variations of glacier changes in the WNT, but could not explain the rapider melting of glaciers in the Nam Co drainage basin.

The glacier area-weighted mean elevation on the side of the Nam Co drainage basin was slightly lower than that of Lhasa River basin (Figure. 2), which may be a possible reason for help explain the rapid glacier ablation this, though even in some comparable elevation bins. However, glacier elevation changes in Nam Co drainage basin were more negative in several elevation bins than in equivalent Lhasa-basin elevations (Figure. 7). Other possible explanations include There might be other reasons for accelerating ice loss, an spatially-variable role for such as black carbon and dust can in reducing the surface albedo of glaciers and thus contribute to their melting (Lau et al., 2010; Ming et al., 2008), and Qu et al. (2014) did observed that a decrease in albedo of the Zhadang glacier in (Nam Co drainage basin) during from 2001–2012.

批注 [HP-B29]: It would also be useful to show the winter versus summer precipitation trends as drier winters, for example, would promote a more negative mass balance.

带格式的: 首行缩进: 0 字符

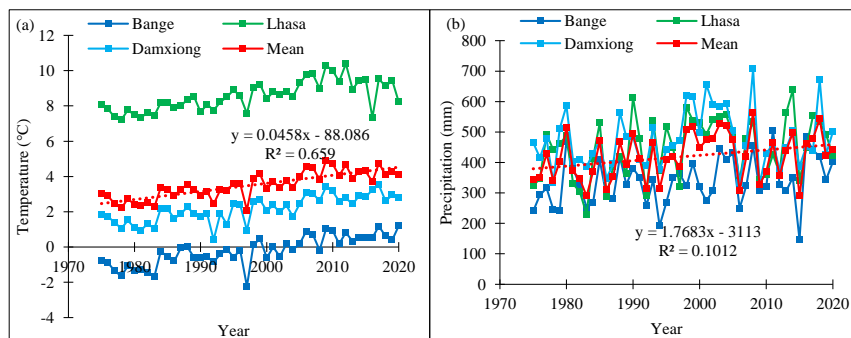


Figure 12 | Annual temperature (a) and precipitation (b) changes for the study area. (a) and (b) Time series of temperature and precipitation at Damxiong, Lhasa and Bange weather stations from 1976 to 2020.

批注 [HP-B30]: See note above about including seasonal temperature and precipitation trends.

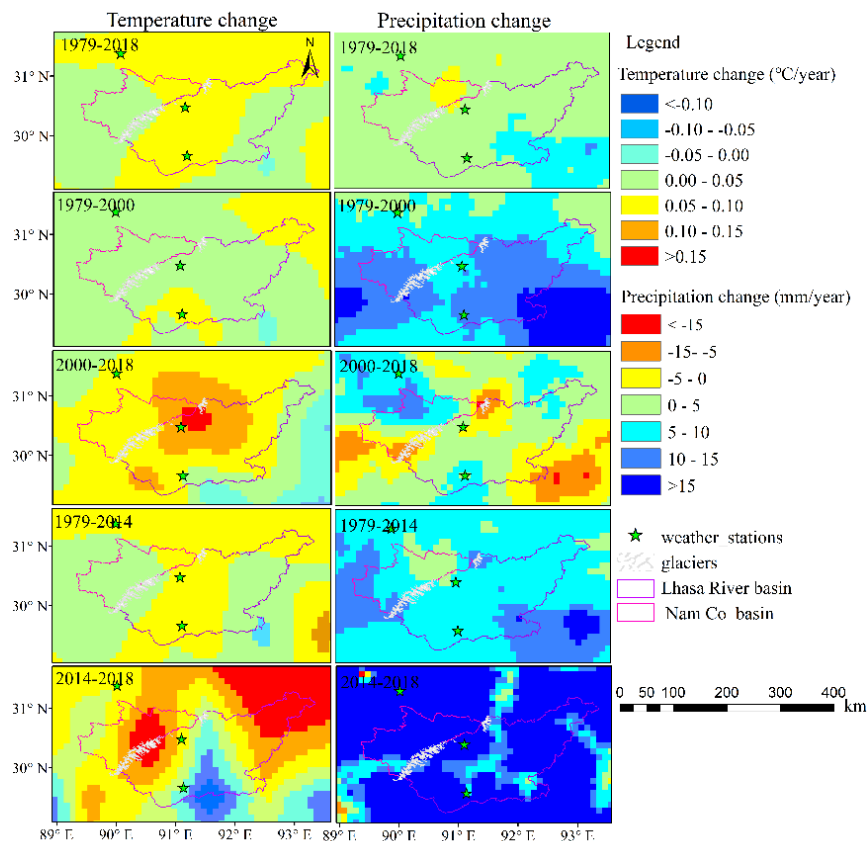


Figure 13 Gridded temperature and precipitation change during specific time periods from China Meteorological Forcing Data.

## 5. Conclusions

Based on the KH-9, Landsat images, SRTM and ASTER satellite data DEMs acquisitions, we have quantified the changes of glacier area, surface elevation changes and mass balance in the WNT during over the past 44 years have been quantified. The Our major conclusions are summarized as follows:

1. (+) Glaciers in the WNT retreat by  $296 \pm 11 \text{ km}^2$ , or 33% of their area, from 1976-2020, at with a mean retreat rate a total area of  $589.17 \pm 34.68 \text{ km}^2$  in 2020. Ice cover has diminished by of  $0.76 \% \text{ a}^{-1}$  since 1976. Over this time, they lost a total of  $11.56 \pm 0.10 \text{ Gt}$  of ice.
2. The average glacier area retreat rate from 2000 to 2020 ( $1.17 \% \text{ a}^{-1}$ ) was more than twice as much as that from 1976 to 2000 ( $0.54 \% \text{ a}^{-1}$ ). Similarly, the mean glacier mass balance from 2000 to 2020 ( $-0.37 \pm 0.15 \text{ m w.e.a}^{-1}$ ) was more negative than that from 1976 to 2000 ( $-0.26 \pm 0.09 \text{ m w.e.a}^{-1}$ ) (though the change is within the uncertainties). Furthermore, the more

批注 [HP-B31]: Enter the area-change uncertainty here.

设置了格式: 字体颜色: 自动设置

设置了格式: 上标

带格式的: 列表段落, 缩进: 左侧: 0 厘米, 悬挂缩进: 5.67 字符, 编号 + 级别: 1 + 编号样式: 1, 2, 3, ... + 起始编号: 1 + 对齐方式: 左侧 + 对齐位置: 1.38 厘米 + 缩进位置: 2.01 厘米

批注 [HP-B32]: Check this total.

设置了格式: 字体颜色: 自动设置

设置了格式: 字体颜色: 自动设置

设置了格式: 字体颜色: 自动设置

设置了格式: 字体颜色: 自动设置

设置了格式: 字体颜色: 自动设置

negative glacier mass balance from 2000 to 2020 was mainly due to the intensified glacier melting after 2014, which was potentially likely associated with significant particularly strong warming of the region after 2014.

3. (2) In the WNT the spatial and temporal heterogeneity patterns of glacier changes loss can be partially largely be explained by the observed patterns of regional climate change. Besides, compared with Locally, the mass balance of varied between different types of glaciers during 1976–2000 with proglacial lakes associated with accelerated glacier melting the most rapid loss, more significantly particularly during 2000–2020, while the inhibition effect of debris cover on glacier melting was weakened. The mass balance of debris-covered glaciers was somewhat more negative than similar to debris-free glaciers during 2000–2020, which indicated an advanced stage of glacier evolution.

4. (3) Topographic setting influenced retreat and thinning, with loss rates decreasing with increasing elevation. The rate of both change of glacier area retreat and thinning and thickness decreased with the increase of elevation, but t. However, the relationship correlation between between the parameters of areal retreat rates and both slope and aspect with thinning rates differed from their relationship with retreat rates, were not consistent spatially and through time. with correlations between thinning rate and slope and aspect. For slopes of 8–40° (including the majority of glaciers), for example, the retreat rate increased with slope while the thinning rate decreased with slope. Furthermore, the relationships between aspect and retreat and thinning varied through time.

In summary, we observed widespread and accelerating glacier loss in the WNT on multi-year time scales, particularly after 2014, associated with altitude and largely explained by changes in regional climate and precipitation. However, factors such as precipitation, temperature and altitude could not yet fully explain the heterogeneity of glacier changes and the specific acceleration points of glacier changes also could not be determined. Thus, more sophisticated remote sensing data and glacier ablation models are needed to fully understand the mechanism of glacier change in the future.

#### References:

- Ali, S., & Khan, G. (2021). *Assessment of glacier status and its controlling parameters from 1990 to 2018 of Hunza Basin, Western Karakorum*.
- Bahr, B., Meier, F., & Peckham, S. D. (1997). The physical basis of glacier volume-area scaling perturbations in the ice mass balance rate  $D$  (rate of ice accumulation area at relatively high elevations low elevations ( $D < 0$  on a yearly average)), Volume-Size. *Journal of Geophysical Research*, 102(B9), 20355–20362.
- Bahr, D. B., Pfeffer, W. T., & Kaser, G. (2015). A review of volume-area scaling of glaciers. *Reviews of Geophysics*, 53(1), 95–140. <https://doi.org/10.1002/2014RG000470>
- Banerjee, A. (2017). Brief communication: Thinning of debris-covered and debris-free glaciers in a warming climate. *Cryosphere*, 11(1), 133–138. <https://doi.org/10.5194/tc-11-133-2017>
- Bhattacharya, A., Bolch, T., Mukherjee, K., King, O., Menounos, B., Kapitsa, V., Neckel, N., Yang, W., & Yao, T. (2021). High Mountain Asian glacier response to climate revealed by multi-temporal satellite observations since the 1960s. *Nature Communications*, 12(1), 1–13. <https://doi.org/10.1038/s41467-021-24180-y>
- Bolch, T., Yao, T., Kang, S., Buchroithner, M. F., Scherer, D., Maussion, F., Huintjes, E., &

设置了格式: 字体颜色: 自动设置

带格式的: 缩进: 首行缩进: 0 厘米

---

Schneider, C. (2010). A glacier inventory for the western Nyainqentanglha range and the Nam Co Basin, Tibet, and glacier changes 1976–2009. *Cryosphere*, 4(3), 419–433.

<https://doi.org/10.5194/tc-4-419-2010>

Brun, F., Wagnon, P., Berthier, E., Jomelli, V., Maharjan, S. B., Shrestha, F., & Kraaijenbrink, P. D. A. (2019). Heterogeneous Influence of Glacier Morphology on the Mass Balance Variability in High Mountain Asia. *Journal of Geophysical Research: Earth Surface*, 124(6), 1331–1345. <https://doi.org/10.1029/2018JF004838>

Brun, Fanny, Berthier, E., Wagnon, P., Kääb, A., & Treichler, D. (2018). A spatially resolved estimate of High Mountain Asia glacier mass balances, 2000–2016. *Nature Geoscience*, 10(9), 668–673. <https://doi.org/10.1038/NGEO2999.A>

Brun, Fanny, Wagnon, P., Berthier, E., Shea, J. M., Immerzeel, W. W., Kraaijenbrink, P. D. A., Vincent, C., Reverchon, C., Shrestha, D., & Arnaud, Y. (2018). Ice cliff contribution to the tongue-wide ablation of Changri Nup Glacier, Nepal, central Himalaya. *Cryosphere*, 12(11), 3439–3457. <https://doi.org/10.5194/tc-12-3439-2018>

Duan, A., & Xiao, Z. (2015). Does the climate warming hiatus exist over the Tibetan Plateau? *Scientific Reports*, 5, 1–9. <https://doi.org/10.1038/srep13711>

Frauenfelder, R., & Kääb, A. (2009). Glacier mapping from multi-temporal optical remote sensing data within the Brahmaputra River Basin. *Proceedings, 33rd International Symposium on Remote Sensing of Environment, ISRSE 2009, 036592(036592)*, 922–925.

Glaciologygeocryology, J. O. F. (2020). *The future changes of Chinese cryospheric hydrology and their impacts on water security in arid areas*.

Guo, W., Liu, S., Xu, J., Wu, L., Shangguan, D., Yao, X., Wei, J., Bao, W., Yu, P., Liu, Q., & Jiang, Z. (2015). The second Chinese glacier inventory: Data, methods and results. *Journal of Glaciology*, 61(226), 357–372. <https://doi.org/10.3189/2015JoG14J209>

He, J., Yang, K., Tang, W., Lu, H., Qin, J., Chen, Y., & Li, X. (2020). The first high-resolution meteorological forcing dataset for land process studies over China. *Scientific Data*, 7(1), 1–11. <https://doi.org/10.1038/s41597-020-0369-y>

Immerzeel, W. W., Lutz, A. F., Andrade, M., Bahl, A., Biemans, H., Bolch, T., Hyde, S., Brumby, S., Davies, B. J., Elmore, A. C., Emmer, A., Feng, M., Fernández, A., Haritashya, U., Kargel, J. S., Koppes, M., Kraaijenbrink, P. D. A., Kulkarni, A. V., Mayewski, P. A., ... Baillie, J. E. M. (2020). Importance and vulnerability of the world's water towers. *Nature*, 577(7790), 364–369. <https://doi.org/10.1038/s41586-019-1822-y>

Kääb, A., Berthier, E., Nuth, C., Gardelle, J., & Arnaud, Y. (2012). Contrasting patterns of early twenty-first-century glacier mass change in the Himalayas. *Nature*, 488(7412), 495–498. <https://doi.org/10.1038/nature11324>

Ke, L., Song, C., Yong, B., Lei, Y., & Ding, X. (2020). Which heterogeneous glacier melting patterns can be robustly observed from space? A multi-scale assessment in southeastern Tibetan Plateau. *Remote Sensing of Environment*, 242(August 2019), 111777. <https://doi.org/10.1016/j.rse.2020.111777>

Lau, W. K. M., Kim, M. K., Kim, K. M., & Lee, W. S. (2010). Enhanced surface warming and accelerated snow melt in the Himalayas and Tibetan Plateau induced by absorbing aerosols. *Environmental Research Letters*, 5(2). <https://doi.org/10.1088/1748-9326/5/2/025204>

Li, G., & Lin, H. (2017). Recent decadal glacier mass balances over the Western Nyainqentanglha Mountains and the increase in their melting contribution to Nam Co Lake

---

measured by differential bistatic SAR interferometry. *Global and Planetary Change*, 149, 177–190. <https://doi.org/10.1016/j.gloplacha.2016.12.018>

Lin, L., Gao, M., Liu, J., Wang, J., Wang, S., Chen, X., & Liu, H. (2020). Understanding the effects of climate warming on streamflow and active groundwater storage in an alpine catchment: The upper Lhasa River. *Hydrology and Earth System Sciences*, 24(3), 1145–1157. <https://doi.org/10.5194/hess-24-1145-2020>

Luo, W., Zhang, G., Chen, W., & Xu, F. (2020). Response of glacial lakes to glacier and climate changes in the western Nyainqentanglha range. *Science of the Total Environment*, 735, 139607. <https://doi.org/10.1016/j.scitotenv.2020.139607>

Lutz, A. F., Immerzeel, W. W., Shrestha, A. B., & Bierkens, M. F. P. (2014). Consistent increase in High Asia's runoff due to increasing glacier melt and precipitation. *Nature Climate Change*, 4(7), 587–592. <https://doi.org/10.1038/nclimate2237>

Maurer, J. M., Schaefer, J. M., Rupper, S., & Corley, A. (2019a). Acceleration of ice loss across the Himalayas over the past 40 years. *Science Advances*, 5(6). <https://doi.org/10.1126/sciadv.aav7266>

Maurer, J. M., Schaefer, J. M., Rupper, S., & Corley, A. (2019b). supplement\_Acceleration of ice loss across the Himalayas over the past 40 years. *Science Advances*, 5(6). <https://doi.org/10.1126/sciadv.aav7266>

Maurer, J., & Rupper, S. (2015). Tapping into the Hexagon spy imagery database: A new automated pipeline for geomorphic change detection. *ISPRS Journal of Photogrammetry and Remote Sensing*, 108, 113–127. <https://doi.org/10.1016/j.isprsjprs.2015.06.008>

Maurer, Joshua M., Rupper, S. B., & Schaefer, J. M. (2016). Quantifying ice loss in the eastern Himalayas since 1974 using declassified spy satellite imagery. *Cryosphere*, 10(5), 2203–2215. <https://doi.org/10.5194/tc-10-2203-2016>

Ming, J., Cachier, H., Xiao, C., Qin, D., Kang, S., Hou, S., & Xu, J. (2008). Black carbon record based on a shallow Himalayan ice core and its climatic implications. *Atmospheric Chemistry and Physics*, 8(5), 1343–1352. <https://doi.org/10.5194/acp-8-1343-2008>

Neckel, N., Kropá, J., Bolch, T., & Hochschild, V. (2014). *Glacier mass changes on the Tibetan Plateau 2003 – 2009 derived from ICESat laser altimetry measurements*. <https://doi.org/10.1088/1748-9326/9/1/014009>

Neckel, Niklas, Loibl, D., & Rankl, M. (2017). Recent slowdown and thinning of debris-covered glaciers in south-eastern Tibet. *Earth and Planetary Science Letters*, 464, 95–102. <https://doi.org/10.1016/j.epsl.2017.02.008>

Nicholson, L., & Benn, D. I. (2006). Calculating ice melt beneath a debris layer using meteorological data. *Journal of Glaciology*, 52(178), 463–470. <https://doi.org/10.3189/172756506781828584>

Nuth, C., & Kääb. (2011). Co-registration and bias corrections of satellite elevation data sets for quantifying glacier thickness change. *Cryosphere*, 5(1), 271–290. <https://doi.org/10.5194/tc-5-271-2011>

Oerlemans and Fortuin. (1992). *Sensitivity of Glaciers and Small Ice Caps to Greenhouse Warming.pdf*.

Pandey, P., Ali, S. N., Ramanathan, A. L., Champati ray, P. K., & Venkataraman, G. (2017). Regional representation of glaciers in Chandra Basin region, western Himalaya, India. *Geoscience Frontiers*, 8(4), 841–850. <https://doi.org/10.1016/j.gsf.2016.06.006>

- 
- Pritchard, H. D. (2019). Asia's shrinking glaciers protect large populations from drought stress. *Nature*, 569(7758), 649–654. <https://doi.org/10.1038/s41586-019-1240-1>
- Qu, B., Ming, J., Kang, S. C., Zhang, G. S., Li, Y. W., Li, C. D., Zhao, S. Y., Ji, Z. M., & Cao, J. J. (2014). The decreasing albedo of the Zhadang glacier on western Nyainqentanglha and the role of light-absorbing impurities. *Atmospheric Chemistry and Physics*, 14(20), 11117–11128. <https://doi.org/10.5194/acp-14-11117-2014>
- Reid, T. D., Carenzo, M., Pellicciotti, F., & Brock, B. W. (2012). Including debris cover effects in a distributed model of glacier ablation. *Journal of Geophysical Research Atmospheres*, 117(17), 1–15. <https://doi.org/10.1029/2012JD017795>
- Ren, S., Menenti, M., Jia, L., Zhang, J., Zhang, J., & Li, X. (2020). Glacier mass balance in the Nyainqentanglha mountains between 2000 and 2017 retrieved from ZiYuan-3 stereo images and the SRTM DEM. In *Remote Sensing* (Vol. 12, Issue 5). <https://doi.org/10.3390/rs12050864>
- RGI Consortium. (2017). *Randolph Glacier Inventory – A Dataset of Global Glacier Outlines: Version 6.0. July*, 1–27. <https://ci.nii.ac.jp/naid/40021243259/>
- Scherler, D., Bookhagen, B., & Strecker, M. R. (2011). Spatially variable response of Himalayan glaciers to climate change affected by debris cover. *Nature Geoscience*, 4(3), 156–159. <https://doi.org/10.1038/ngeo1068>
- Shangguan, Donghui;Liu, Shiyin;Ding, L. (n.d.). *Variation of Glaciers in the Western Nyainqentanglha Range of Tibetan Plateau during 1970–2000*.
- Shiqiang Zhang, Xin Gao, Baisheng Ye, X. Z. and S. H. (2011). *A modified monthly degree-day model for evaluating glacier runoff changes in China. Part II: application*. 2274(November 2008), 2267–2274. <https://doi.org/10.1002/hyp>
- Su, F., Zhang, L., Ou, T., Chen, D., Yao, T., Tong, K., & Qi, Y. (2016). Hydrological response to future climate changes for the major upstream river basins in the Tibetan Plateau. *Global and Planetary Change*, 136, 82–95. <https://doi.org/10.1016/j.gloplacha.2015.10.012>
- Surazakov, A., & Aizen, V. (2010). Positional accuracy evaluation of declassified hexagon KH-9 mapping camera imagery. *Photogrammetric Engineering and Remote Sensing*, 76(5), 603–608. <https://doi.org/10.14358/PERS.76.5.603>
- Thompson, S. S., Benn, D. I., Dennis, K., & Luckman, A. (2012). A rapidly growing moraine-dammed glacial lake on Ngozumpa Glacier, Nepal. *Geomorphology*, 145–146, 1–11. <https://doi.org/10.1016/j.geomorph.2011.08.015>
- Vincent, C., Wagnon, P., Shea, J. M., Immerzeel, W. W., Kraaijenbrink, P., Shrestha, D., Soruco, A., Arnaud, Y., Brun, F., Berthier, E., & Sherpa, S. F. (2016). Reduced melt on debris-covered glaciers: Investigations from Changri Nup Glacier, Nepal. *Cryosphere*, 10(4), 1845–1858. <https://doi.org/10.5194/tc-10-1845-2016>
- Viviroli, D., Dürr, H. H., Messerli, B., Meybeck, M., & Weingartner, R. (2007). Mountains of the world, water towers for humanity: Typology, mapping, and global significance. *Water Resources Research*, 43(7), 1–13. <https://doi.org/10.1029/2006WR005653>
- Wang et al., 2012. (n.d.). *Glacier temporal- spatial change characteristics in western Nyainqentanglha Range, Tibetan Plateau 1977-2010*.
- Wang, J., Chen, X., Liu, J., Hu, Q., & Sciences, A. (n.d.). *Changes of Precipitation–Runoff Relationship Induced by Climate Variation in a Large Glaciated Basin of the Tibetan Plateau*. <https://doi.org/10.1029/2020JD034367>
- Wang, Q., Yi, S., & Sun, W. (2021). Continuous Estimates of Glacier Mass Balance in High

---

Mountain Asia Based on ICESat-1,2 and GRACE/GRACE Follow-On Data. *Geophysical Research Letters*, 48(2). <https://doi.org/10.1029/2020GL090954>

Wu, G., Duan, A., Liu, Y., Mao, J., Ren, R., Bao, Q., He, B., Liu, B., & Hu, W. (2015). Tibetan Plateau climate dynamics: Recent research progress and outlook. *National Science Review*, 2(1), 100–116. <https://doi.org/10.1093/nsr/nwu045>

Wu, Kun peng, Liu, S. yin, Guo, W. qin, Wei, J. feng, Xu, J. li, Bao, W. jia, & Yao, X. jun. (2016). Glacier change in the western Nyainqentanglha Range, Tibetan Plateau using historical maps and Landsat imagery: 1970–2014. *Journal of Mountain Science*, 13(8), 1358–1374. <https://doi.org/10.1007/s11629-016-3997-0>

Wu, Kunpeng, Liu, S., Jiang, Z., Xu, J., & Wei, J. (2019). Glacier mass balance over the central Nyainqentanglha Range during recent decades derived from remote-sensing data. *Journal of Glaciology*, 65(251), 422–439. <https://doi.org/10.1017/jog.2019.20>

Wu, Kunpeng, Liu, S., Jiang, Z., Xu, J., Wei, J., & Guo, W. (2018). Recent glacier mass balance and area changes in the Kangri Karpo Mountains from DEMs and glacier inventories. *Cryosphere*, 12(1), 103–121. <https://doi.org/10.5194/tc-12-103-2018>

Wu, Y., & Zhu, L. (2008). The response of lake-glacier variations to climate change in Nam Co Catchment, central Tibetan Plateau, during 1970–2000. *Journal of Geographical Sciences*, 18(2), 177–189. <https://doi.org/10.1007/s11442-008-0177-3>

Yang, K., & He, J. (2019). China meteorological forcing dataset (1979–2018). In N. T. P. D. Center (Ed.), *National Tibetan Plateau Data Center*. National Tibetan Plateau Data Center. <https://doi.org/10.11888/AtmosphericPhysics.tpe.249369.file>

Yang, K., He, J., Tang, W., Qin, J., & Cheng, C. C. K. (2010). On downward shortwave and longwave radiations over high altitude regions: Observation and modeling in the Tibetan Plateau. *Agricultural and Forest Meteorology*, 150(1), 38–46. <https://doi.org/10.1016/j.agrformet.2009.08.004>

Yao-jun, L. I., Yong-jian, D., Dong-hui, S., & Rong-jun, W. (2020). ScienceDirect Regional differences in global glacier retreat from 1980 to 2015. *Advances in Climate Change Research*, 10(4), 203–213. <https://doi.org/10.1016/j.accre.2020.03.003>

Yao, T. D., Li, Z. G., Yang, W., Guo, X. J., Zhu, L. P., Kang, S. C., Wu, Y. H., & Yu, W. S. (2010). Glacial distribution and mass balance in the Yarlung Zangbo river and its influence on lakes. *Chinese Science Bulletin*, 55(20), 2072–2078. <https://doi.org/10.1007/s11434-010-3213-5>

Yao, T., Pu, J., Lu, A., Wang, Y., & Yu, W. (2007). Recent glacial retreat and its impact on hydrological processes on the Tibetan Plateau, China, and surrounding regions. *Arctic, Antarctic, and Alpine Research*, 39(4), 642–650. [https://doi.org/10.1657/1523-0430\(07-510\)\[YAO\]2.0.CO;2](https://doi.org/10.1657/1523-0430(07-510)[YAO]2.0.CO;2)

Yao, T., Thompson, L., Yang, W., Yu, W., Gao, Y., Guo, X., Yang, X., Duan, K., Zhao, H., Xu, B., Pu, J., Lu, A., Xiang, Y., Kattel, D. B., & Joswiak, D. (2012). Different glacier status with atmospheric circulations in Tibetan Plateau and surroundings. *Nature Climate Change*, 2(9), 663–667. <https://doi.org/10.1038/nclimate1580>

Ye, Q., Zong, J., Tian, L., Cogley, J. G., Song, C., & Guo, W. (2017). Glacier changes on the Tibetan Plateau derived from Landsat imagery: Mid-1970s - 2000-13. *Journal of Glaciology*, 63(238), 273–287. <https://doi.org/10.1017/jog.2016.137>

Yu, W., Yao, T., Kang, S., Pu, J., Yang, W., Gao, T., Zhao, H., Zhou, H., Li, S., Wang, W., & Ma, L. (2013). Different region climate regimes and topography affect the changes in area and



---

mass balance of glaciers on the north and south slopes of the same glacierized massif (the West Nyainqentanglha Range, Tibetan Plateau). *Journal of Hydrology*, 495, 64–73.  
<https://doi.org/10.1016/j.jhydrol.2013.04.034>

Zhang, G., Yao, T., Shum, C. K., Yi, S., Yang, K., Xie, H., Feng, W., Bolch, T., Wang, L., Behrangi, A., Zhang, H., Wang, W., Xiang, Y., & Yu, J. (2017). Lake volume and groundwater storage variations in Tibetan Plateau's endorheic basin. *Geophysical Research Letters*, 44(11), 5550–5560. <https://doi.org/10.1002/2017GL073773>

Zhang, Q., & Zhang, G. (2017). Glacier elevation changes in the western nyainqentanglha range of the Tibetan Plateau as observed by TerraSAR-X/TanDEM-X images. *Remote Sensing Letters*, 8(12), 1142–1151. <https://doi.org/10.1080/2150704X.2017.1362123>

Zhao, Q., Ding, Y., Wang, J., Gao, H., Zhang, S., Zhao, C., Xu, J., Han, H., & Shangguan, D. (2019). Projecting climate change impacts on hydrological processes on the Tibetan Plateau with model calibration against the glacier inventory data and observed streamflow. *Journal of Hydrology*, 573(December 2018), 60–81. <https://doi.org/10.1016/j.jhydrol.2019.03.043>

Zhou, S., Kang, S., Chen, F., & Joswiak, D. R. (2013). Water balance observations reveal significant subsurface water seepage from Lake Nam Co, south-central Tibetan Plateau. *Journal of Hydrology*, 491(1), 89–99. <https://doi.org/10.1016/j.jhydrol.2013.03.030>

Zhou, Y., Hu, J., Li, Z., Li, J., Zhao, R., & Ding, X. (2019). Quantifying glacier mass change and its contribution to lake growths in central Kunlun during 2000–2015 from multi-source remote sensing data. *Journal of Hydrology*, 570(January), 38–50.  
<https://doi.org/10.1016/j.jhydrol.2019.01.007>

Zhou, Y., Li, Z., Li, J., Zhao, R., & Ding, X. (2018). Glacier mass balance in the Qinghai–Tibet Plateau and its surroundings from the mid-1970s to 2000 based on Hexagon KH-9 and SRTM DEMs. *Remote Sensing of Environment*, 210(March 2017), 96–112.  
<https://doi.org/10.1016/j.rse.2018.03.020>